RUSSIAN JOURNAL OF EARTH SCIENCES, VOL. 6, NO. 4, PAGES 257–277, AUGUST 2004

Elbrus active Volcano and its geological history

A. G. Gurbanov[1], V. M. Gazeev[1], O. A. Bogatikov[1], V. B. Naumov[2], A. Ya. Dokuchaev[1] and A. V. Shevchenko[3]

Abstract. Using the new geological map of the Elbrus Volcano (scale 1:50 000) and the new isotopic datings of the volcanic rocks, the formation history of Elbrus Volcano was found to include a pre-caldera, a caldera, and a post-caldera cycle, during which the modern Elbrus stratovolcano was formed. The Early and The Late period of the volcano's evolution have been identified in the two latter cycles.

Introduction

A principally new geological map of the Elbrus stratovolcano was compiled on the scale of 1:50000 (Figure 1) as a result of detailed geological studies combined with the interpretation of air photographs and space images, isotope and EPR dating (electronic paramagnetic resonance using rock-forming quartz), and mapping individual lava flows, tuff and ignimbrite horizons, as well as breaks in volcanic activity, represented by moraine deposits resting on the surface of lava flows in the same volcanic rock sequence. This map shows that the formation history of the Elbrus Volcano included a pre-caldera cycle, a caldera cycle, the onset of which was marked by a powerful explosive eruption, responsible for the caldera formation, and a post-caldera cycle which resulted in the formation of the present-day Elbrus stratovolcano. It is important to note that each of the two latter cycles included The Early and The Late period of the evolution of the volcano.

No pre-caldera volcanic rocks have been found confidently thus far. These are supposed to include the outliers of trachyandesite lava flows found in the mouth of the Khudes River (up to 200 m thick) and of trachybasalt lava flows (120–150 m thick) in the upper reaches of the Tyzyl River. According to one whole-rock sample, the K-Ar age of the Khudes trachyandesite was found to be 800 thousand years old [*Borsuk,* 1979]. Because the rocks of this cycle are as far as a few tens of kilometers away from the stratovolcano, they are not shown in the geological map of this scale.

The caldera-type volcanic activity had been associated with the formation of the Elbrus large collapse caldera, mapped by *Bogatikov et al.* [1998b], and measuring 17×14 km along the edge of the scarp limiting it. Associated with the formation of this caldera were the voluminous ejections of rhyodacite and rhyolite pyroclastic materials and the formation of tuff and ignimbrite covers. The formation of the caldera was dated by the K-Ar method using glass and the poorly crystallized ground mass of biotite ignimbrite with pink quartz. Outside of the caldera this ignimbrite composes a fairly thick (up to 200–250 m) nappe located 20 km WNW of the Elbrus Volcano in the upper reaches of the Chuchkhur River. The resulting age of 790±70 thousand years seems to date the voluminous explosive eruptions. These data suggesting the Early Neopleistocene age of the beginning of the caldera formation cycle have been supported by another independent method, namely, by U-Pb SHRIMP zircon measurements using zircons extracted from the ignimbrite fiamme in the area of the Chuchkhur River (689±30 thousand years) and also in the area of the Kyukyurtly Glacier (722±15 thousand years). Ignimbrites with columnar jointing are exposed in the right side of the Kyukyurtly R. Valley, where the background shows an old crater with a large subvolcanic dacite body intruded into it (Figure 2).

The Late Pleistocene-Holocene cone of the Elbrus stratovolcano standing inside the caldera is composed mainly of dacite lava breccias and rhyolite tuff. The Eastern and Western summit craters are crossed by a sublatitudinal, obviously magma controlling fault zone (Syltran Fault) which is marked by a number of small volcanic cones in the Kyrtyk, Syltran-Su, Biitik-Tebe, and other river valleys (Figure 3).

[1] Institute of Geology of Ore Deposits, Petrography, Mineralogy and Geochemistry, Russian Academy of Science, Moscow, Russia
[2] Vernadsky Institute of Geochemistry and Analytical Chemistry, Moscow, Russia
[3] Kabardino-Balkarian University

Copyright 2004 by the Russian Journal of Earth Sciences.

Paper number TJE04153.
ISSN: 1681–1208 (online)

The online version of this paper was published 15 September 2004.
URL: http://rjes.wdcb.ru/v06/tje04153/tje04153.htm

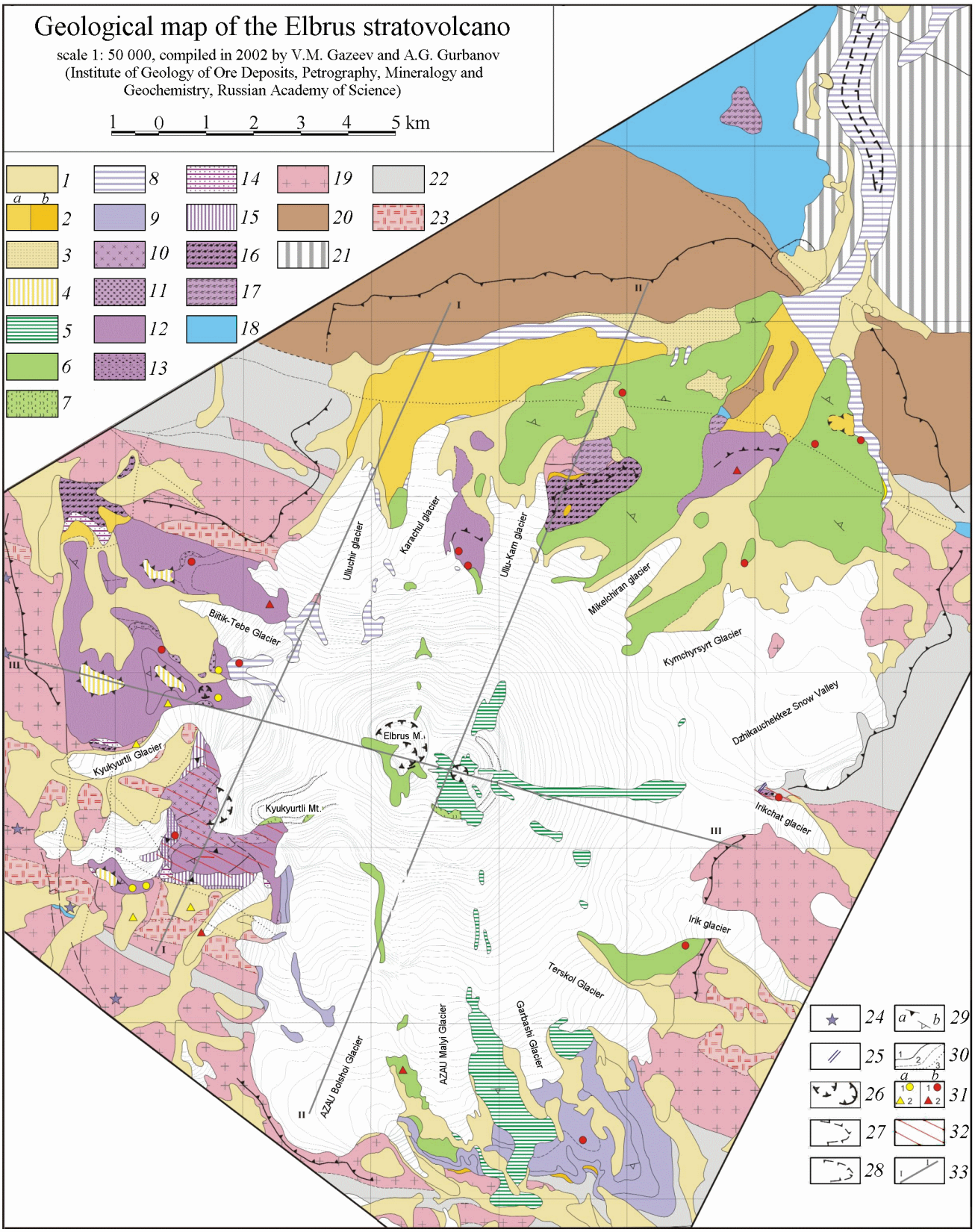
Geological map of the Elbrus stratovolcano
scale 1: 50 000, compiled in 2002 by V.M. Gazeev and A.G. Gurbanov
(Institute of Geology of Ore Deposits, Petrography, Mineralogy and
Geochemistry, Russian Academy of Science)
1 0 1 2 3 4 5 km
1 a b
2
3
4
5
6
7
8
9
10
11
12
13
14
15
16
17
18
19
20
21
22
23
24
25
26
27
28
29 a b
30 a b
31
32
33
Ullu-tchir glacier
Karachul glacier
Ullu-Kam glacier
Mikelchiran glacier
Kymchyrsyrt Glacier
Dzhikauchekkez Snow Valley
Irikchat glacier
Irik glacier
Terskol Glacier
Garbashi Glacier
AZAU Malyi Glacier
AZAU Bolshoi Glacier
Biitik-Tebe Glacier
Kyukyurtli Glacier
Kyukyurtli Mt.
Elbrus M.
I
II
III

The Elbrus Volcano is restricted to the area where the Syltran magma-controlling fault zone is intersected by the Elbrus transverse fault zone, where it rests on old crystalline rocks occurring as a horst block. The diameter of the volcano's base is about 14–15 km, the relative height of the volcano being 3 km (Figure 4). The western and eastern peaks, as well as the whole cone of the volcano, are restricted to a huge collapse caldera measuring about 230 km^2 in area [*Bogatikov et al.,* 1998b].

The structural details of this volcanic cone are discussed below. The only comment here is that most of the Elbrus lava flows are composed of dacite, whereas the ignimbrites, lavas, and tuffs are composed of rhyodacite (see "Early Caldera-Cycle Volcanic Rocks" section).

Figure 2. Ancient crater with a large subvolcanic dacite body intruded into it (source area of the Kyukyurtly R.)

Pre-Caldera Volcanic Activity

We interpreted conventionally as pre-caldera volcanic rocks the oldest trachybasaltic andesite lava flow outliers (totaling 150 m in thickness) outcropping in the area of the Tyzyl R. upper reaches (36 km NNE of Elbrus). The outliers of these lava flows rest 400–450 m higher above the modern river channel. This allowed us to use geomorphologic data for dating them as Late Pleistocene–Early Quaternary. In addition, the Elbrus Neopleistocene and Holocene lava flows contain inclusions which are similar in composition to the Tysyl River trachybasaltic andesite, even though no lava flows of this composition have been found in the Elbrus volcanic cone. On this basis the rocks in question have been ranked as pre-caldera formations.

Also interpreted as pre-caldera rocks were the outliers of a trachyandesite lava flow, up to 200 m thick, with a K-Ar age of 800±250 thousand years [*Borsuk,* 1979], exposed in the left side of the Khudes R. Valley, in its mouth, that is, 40 km northwest of Elbrus. It is important to note that these volcanic rocks are localized in a tectonically downthrown block (roughly to a distance of 250 m), their base resting now at an elevation of 200 m above the modern channel of the river. Consequently, taking into account the vertical magnitude of the displacement along this fault, the bottom of this lava flow should have resided now at an altitude of about 450 m above the modern channel of the Khudes River, this providing a geomorphologic criterion for ranking it as a Late Pleistocene–Quaternary formation.

It should be noted that the scale (1:50 000) of the geological map of the Elbrus volcanic center did not allow us to show the pre-caldera rocks in it.

Figure 1. Geological map of the Elbrus stratovolcano, scale 1: 50 000, compiled in 2002 by V.M. Gazeev and A.G. Gurbanov (Institute of Geology of Ore Deposits, Petrography, Mineralogy and Geochemistry, Russian Academy of Science).
Legend to the map: (1–2) moraines and fluvioglacial deposits: (1) historical and recent, (2a) Late Pleistocene, (2b) Early-Middle Pleistocene, (3) dammed lake deposits, (4) planation surface with relicts of a moraine and fluvioglacial deposits of Pleistocene age, (5–17) volcanic rocks: (5) Late Holocene trachydacite, (6) Early Holocene dacite and trachydacite, (7) Late Pleistocene-Holocene tuff and tufflava, (8, 9) Middle and Late Pleistocene lava flows, (10–17) caldera volcanic rocks: (10) Kyukyurtly extrusion, (11) small extrusive bodies, (12) lava flows, (13) tuff breccia and slag, (14–16) Early Pleistocene: (14) tufflava, tuff, and pumice; (15) rhyodacite lava and agglomerate flows, (16) ignimbrite and tuff of rhyodacite and dacite composition, (17) Late Pliocene ignimbrite and tuff of rhyodacite composition, (18–23) the rocks of the volcanic basement: (18) Lower Jurassic gravelstone, sandstone, and siltstone; (19) Middle Paleozoic volcanic and volcano-sedimentary rocks, (20) Middle Paleozoic crystalline schist, (21) Late Paleozoic granite, (22) crystalline schist and gneiss of the Makera Series, (23) migmatite; (24) necks, (25) felsite porphyry dike, (26) volcanic crater, (27) outline of relict planation surface, (28) outline of erosion window, (29) dip and strike: (a) dip of rocks, (b) flow direction, (30) geological boundaries: (1) proved, (2) inferred), (3) unexposed, (31) sites of hydrothermal activity: (a) of magnesite composition, (b) of siliceous-aluminous and siliceous composition: (1) found in situ, (2) fragments slightly removed from the source, (32) Argillization, (33) The sections along the lines I-I, II-II, III-III; Names in the map: (1) Biitik-Tebe Glacier, (2) Ulluchir, Karachul, and Ullu-Kam glaciers, (3) Mikelchiran, Irikchat, and Irik glaciers, (4) Terskol, Garbashi, and AZLU Malyi Glacier, (5) AZLU Bolshoi Glacier, (6) Kyukyurtli Mt., (7) Elbrus M., (8) Dzhikauchekkez Snow Valley.

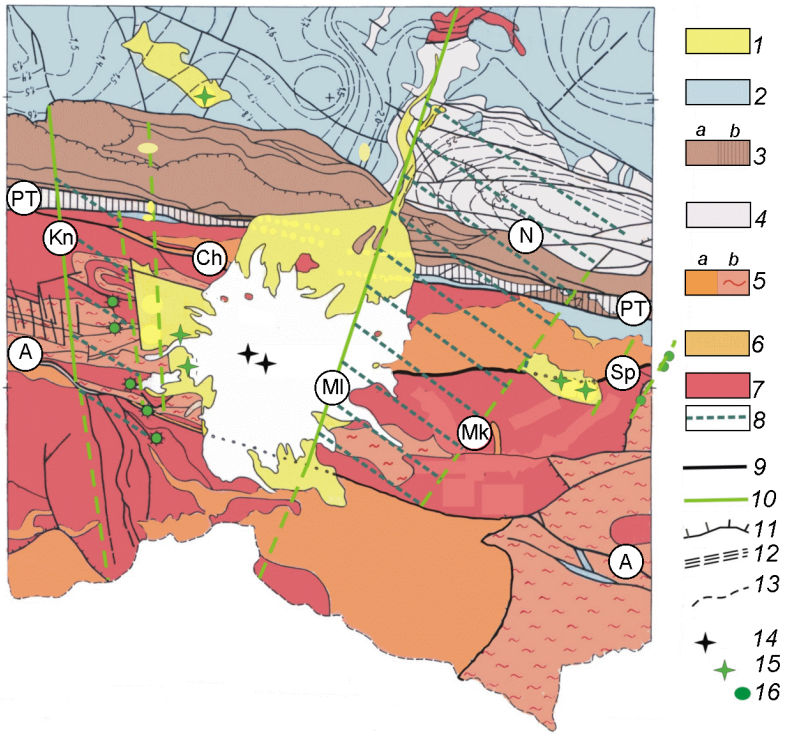

Figure 3. Structural and tectonic map for the area of the Elbrus volcanic center, Scale 1:200 000. Legend to the map: Rock-structure complexes; (1) Alpine structural stage: rhyolite, rhyodacite, and dacite (Q); (2) Cimmerian structural stage: sandstone, siltstone, and argillite (J_{1-2}); Pre-Mesozoic structural stage; (3) Forerange (a) grey (C_{2-3}) and red (P_1) molasses, island-arc sedimentary and volcanic rocks (D-C_1), (b) metamorphic crystalline schist (PR_2); (4) Bechasy anticlinal zone: sedimentary and volcanic rocks of the Khasaut Series (PR_2) and crystalline schists of the Shaukamnysyrt metamorphic rock series (PR_2); (5) Main Ridge (a) crystalline schists of the Makera metamorphic series; (b) migmatite and gneiss of the Gondarai metamorphic complex (PR_2). (6) Intrusive rock complexes: intrusions of the Elbrus-Kazbek Complex (undifferentiated); (7) Malka, Ullu-Kam, and Belorechensk granite complexes (undifferentiated) (Pz_{2-3}). (8) Zones showing a stable tendency toward recent rising. Faults: (9) regional faults: (N) Northern Fault, (PT) Pshekish-Tyrnyauz, (Sp) Syptransut, (Ch) Chemartkol, and (A) Adylsu; (10) recent faults: (Kn) Kichkinikolskii, (Ml) Malkinskii, (Mk) Mkyarskii; (11) overthrusts; (12) junction zones of transverse blocks with different evolution trends; (13) structure contour line. Volcanic apparatuses: (14) Holocene, (15) Preholocene, (16) necks and eroded feeders.

Early Caldera-Cycle Volcanic Rocks

Ignimbrite and Associated Tuff

The ignimbrite and associated tuff occur in small areas (less than 1.1 km^2) or as scattered outliers. According to the geological data observed, we ranked them as the products of the early caldera-formation activity. The ignimbrite area is displaced to the north relative to the Neopleistocene and Holocene volcanic rock sequences of Elbrus and is not controlled by the boundaries of the caldera scarp. The analysis of the preserved fragments of this rock sequence suggests some time gap between these events and the subsequent period of the formation of the later Elbrus caldera which had been mapped earlier using geomorphologic evidence [*Bogatikov et al.,* 1998b].

As to the inner area of the caldera, the outcrops of ignimbrite and associated tuff have been mapped in the right-hand side of the Kyukyurtly R. Valley, in the source area of the Biitik-Tebe River, near the Ullu-Maliendurku Glacier ("Aerodrome" site), in the right-hand side of the Birdzhali-Su R. Valley, and near the Irik Pass. In the area beyond the caldera step, these rocks are known in the right side of the valley of the Birdzhali-Su River and in the area of the Irik Pass. As to the areas beyond the caldera scarp, they are known in the Tuzluk Mountain, in the source area of the Chemartkol R., and in the lower part of the Biitik-Tebe R. Valley. The stratigraphic position of these rocks is identical everywhere. They occur only at the base of the volcanic structure and have not been found anywhere higher. Their thick and most informative sequences are preserved only in the source area of the Kyukyurtly River, in the right-hand side of the valley, opposite the Kyukyurtly Glacier, and in the upper reaches of the Biitik-Tebe River (in a narrow graben of a meridional strike). The most complete rock se-

quence in the Kyukyurtly R. Valley shows that the Late Paleozoic granite pedestal is overlain in fragments by a layer (less than 10 m thick) composed of poorly cemented angular and poorly rounded fragments of Paleozoic crystalline rocks of the Main Caucasus Range zone. Successively following upward is a 60–80-meter layer of dark gray ignimbrite showing well expressed columnar jointing and a 10–20-meter member of light gray rhyodacite tuff with pink quartz phenocrysts and containing no small black glass lenses in contrast to the underlying ignimbrite. Where the top of this rock sequence is preserved, it includes a light gray to white volcaniclastic rock layer (up to 10–12 m thick) of ash-pumice composition. It should be noted that outwardly the above ignimbrite resembles that of the Chemartkol R. area and the less baked tuff from the Tuzluk Mountain and from the Ullu-Maliendurku Glacier, known as the "Aerodrome" area in the source area of the Malka River. Of greatest interest in this rock sequence is ignimbrite. Its appearance in volcanic rock sequences usually suggests past catastrophic explosive events.

Let us consider briefly the internal structure of the ignimbrite sequence in the above-mentioned area. In the bottom and top of this sequence the ignimbrite is represented by its ash-gray baked, thin-plated variety (not more than 5–10 m thick) with lenticular black glass inclusions. This material grades slowly to a pinkish-gray compact, notably fluidal rock variety exposed in the central part of the sequence. Typical of this rock sequence is the fiamme-type orientation of the glass inclusions. The rock has an ignimbrite and locally a pipernoid microstructure, its pseudoflow texture being produced by the distinct orientation (flow) of a fine-grained intermediate glassy material. The rock consists of whole crystals and their fragments, fiamme, and lithoclasts enclosed in an ash mass. The phenocrysts and their fragments are composed of plagioclase, biotite, quartz, and less frequent pyroxene. The fiamme has a characteristic flat form with broken contacts and contains the same set of phenocrysts immersed in the same glassy material as the ignimbrite. The internal structure of the fiamme is feather-like, radially fibrous, and less common comb-like with an elongated void in the central part of a flat lens.

Plagioclase is represented by oligoclase or oligoclase-andesine and is present in the form of fragments (less than 1.5 mm in size) and occasional whole zoned broad tabular crystals (up to 2.5–3 mm in size), usually grown together with biotite.

Biotite usually occurs in the form of plates or scales, less than 1.5 mm in size, which are often differentiated and have normal or indistinct end limitations. This mineral is usually fresh, yet can be opacitized and often contains apatite inclusions.

Quartz occurs as subisometric corroded crystals and their fragments. In some areas (Irik Pass) superposed quartz was found in the form of thin, comb-like veinlets.

The lithoclasts are represented by the fragments of the rocks that compose the basement and of the effusive rocks which have not been encountered in the sections that crossed the Elbrus volcanic cone.

The mesostasis is a brownish glassy pseudofluidal and occasionally slightly devitrified rock mass showing the formation of a spherolitic texture. These rocks agree almost wholly with the classical description of ignimbrite given by *Sheimovich* [1979].

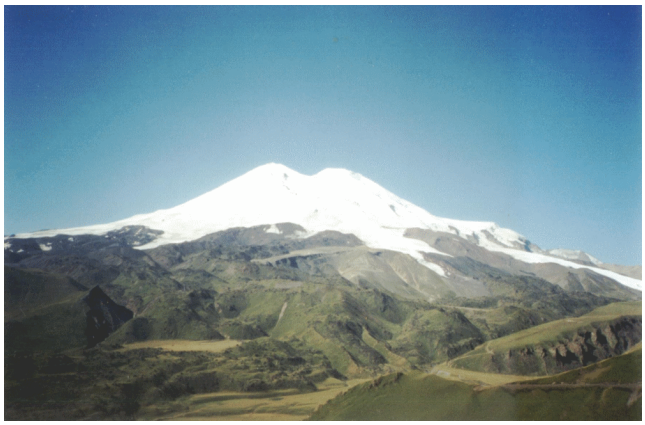

Figure 4. General view of Elbrus stratovolcano from the north, from the Malka River.

Considering the geomorphologic criteria used to date ignimbrite sequences, it should be specified that these criteria should be used with due regard for the tectonic specifics of the area [*Stankevich,* 1976]. In this approach the most correct data are those of ignimbrite outcrops that occur beyond the limits of a caldera scarp. In the areas of the Tuzluk Mt. and Chemartkol R. the base of the ignimbrite sequence resides at a relative elevation of 350–400 m above the modern channels of the Malka and Chemartkol rivers. These elevations agree with the elevations of 370–400 m for the highest outcrops of the ignimbrites (outside of the caldera) in the right-hand side of the Biitik-Tebe R. Valley [*Koronovskii,* 1968]. It should be noted however that the bulk of the ignimbrite sequence in the Biitik-Tebe R. Valley reside at relatively lower elevations of 50–60 m above the present-day course of the river, yet, in some downthrown blocks it had not been exposed down to its base, that is, had not been cut by the river. This seeming contradiction calls for a special discussion, because this low position of the Biitik-Tebe ignimbrite base was used by some investigators [*Koronovskii,* 1968 and others], to name merely one reference, as a basis for ranking these rocks to be younger than the ignimbrites exposed in the valleys of the other rivers mentioned above. Consequently, following the ingnimbrites, the entire sequence of the Biitik-Tebe volcanic rocks had been drastically rejuvenated and stratified in the wrong way in the consequitive succession of the lava flows erupted by the Elbrus Volcano.

Earlier, we mentioned the effect of the tectonic factor proved in the western part of the Elbrus-Kyukyurtly volcanic cone and represented by caldera-forming faults and also by pre-caldera narrow grabens of a meridional strike. One of the arguments that proves the older age of the Biitik-Tebe ignimbrite (compared to the age proposed by *Koronovskii* [1968]), and of all overlying volcanic rocks, is the presence of the relics of the denudation surfaces with scarce rounded pebbles of the rocks from the zone of the Main Caucasus Ridge, which we discovered on the surface of the Biitic-Tebe

Table 1. Contents of petrogenic and trace elements in the rocks of the early caldera cycle: Ignimbrites and associated tuff

Component	Sample number						
	59k/97	54-1/97	52g/98	85/98a	49g/98	93/98	95/98
SiO_2	70.5	66.9	67.8	67	68.7	65.85	66.05
TiO_2	0.5	0.63	0.65	0.65	0.65	0.7	0.8
Al_2O_3	14.8	15.5	15.5	15.5	14.9	15.2	15.1
Fe_2O_3	0.35	1.06	1.18	0.82	1.44	1.42	0.67
FeO	1.8	2.67	2.13	2.57	1.56	1.92	2.78
MnO	0.032	0.051	0.072	0.086	0.054	0.075	0.073
MgO	0.91	1.06	1.36	1.95	1.46	1.06	1.05
CaO	2.37	2.74	2.5	3.09	1.83	3.2	3.19
Na_2O	3.79	3.72	3.99	4.17	3.76	3.08	3.63
K_2O	3.98	3.33	3.55	3.16	4	3.6	3.32
P_2O_5	0.16	0.15	0.26	0.17	0.11	0.19	0.19
H_2O	0.28	0.39	0.05	0.07	0.32	0.62	0.8
CO_2	0.11	0.07					
Total	99.582	98.271	99.042	99.23	98.784	96.915	97.653
Cr	20	29	38	40	28	37	30
Ni	28	20	17	22	20	27	15
Co	4.7	6.4	10.3	9.2	5.8	7.4	6.6
Sc	5.2	5.5	7.7	8.4	5.6	6.8	6.7
Cu	7	8	7	8	15	0	10
Pb	12	60	13	13	13	6	14
Zn	57	66	59	54	45	76	60
W	2	2.8	0.5	0.8	0.7	0.8	0.7
Mo	1.6	1.8	10.5	8.1	8.5	7.7	9.1
As	15.2	7.1	8.9	6.5	14.1	9.2	8
Se	1.7	0.8	2.1	0.5	1.7	1.5	1.9
Sb	0.2	6.8	0.3	0.4	0.6	1.4	0.4
Ag	202	184	157	128	215	160	157
Rb	10.1	19.3	13.3	6.6	19.1	23.4	12.1
Cs	468	329	92	523	535	454	479
Ba	252	298	296	310	241	287	294
Sr	24	25	17	14	16	14	18
Ga	1.2	1.16	1.32	0.79	1.2	0.99	1.06
Ta	5	4.8	6.2	5.6	5.1	5.2	5.3
Hf	248	262	179	161	119	182	160
Zr	2130	3047	2990	3043	2397	2185	2665
Ti	21	29	10	10	15	9	11
Y	26.4	21.3	27.1	21.2	25.5	20.4	21.5
Th	5.8	5.3	6	3.7	5.1	4.2	4.7
U	36.4	39.4	46.7	46.6	48.9	48.1	46.8
La	63.2	69.9	83.9	72.7	75.6	71.4	72.6
Ce	38	34	41	35	36	37	38
Nd	4.94	4.95	6.29	5.07	5.43	5.2	5.13
Sm	0.92	0.98	1.22	1.08	0.97	1.07	1.06
Eu	0.53	0.61	0.68	0.51	0.45	0.43	0.53
Tb	1.5	1.5	1.6	1.4	0.45	1.3	1.2
Yb	0.21	0.06	0.16	0.16	0.14	0.17	0.13
Lu	0.1	0.08	0.07	0.09	0.07	0.1	0.056

dacite lavas. The absolute elevation marks of these surfaces are 3350 m in the left side of the Kyukyurtly R. Valley and 3650–3700 m in the water-divide area between the Biitik-Tebe and Kyukyurtly rivers, their relative elevations above the channels of modern rivers being greater than 300 m. Consequently, relying only on the geomorphology and neglecting the tectonic effects, one can get different age values for the same rock sequence. At the same time using tectonic evidence and new geomorphologic data, the age of the ignimbrite and of the overlying Biitic-Tebe volcanic rocks can be estimated more correctly. For instance, *Dotduev* [1975, 1981] reported that the ages of the erosion and erosion-denudation levels rising 250–300 m and 450–500 m above the modern Baksan River course (in the area north of Tyrnyauz City) date the floors of the Early-Middle Pleistocene (Q_{1-2}) and Late Pleistocene (N_2ap-a) river valleys, respectively.

Consequently, the geomorphologic data suggest that the oldest ages of the ignimbrite and associated tuff are not older than Early Neopleistocene (Q_1). This conclusion agrees with the data reported by *Stankevich* [1976] who found that

the rocks of the Elbrus Volcano had direct magnetic polarity, corresponding generally to the Brunhes Epoch (0–700 thousand years). Using the K-Ar method and the mesostatic glassy groundmass, with all biotite scales and plagioclase and pyroxene phenocrysts removed, we got the age of 790±70 thousand years. The age of 689±30 thousand years was obtained by the U-Pb SHRIMP measurements of zircons from the fiamme in the Chemartkol R. ignimbrite outside of the caldera. These values turned out to be close to the inferred ages. It is important to mention that the optical and electron-microscopic studies of ignimbrite thin sections proved the presence of the macrofragments (a few centimeters) and microparticles (hundredth fractions of a millimeter) in the ignimbrites, which might have caused somewhat older K-Ar age values.

The chemical compositions of the rocks of the early caldera cycle and of the contents of metallic, rare, and disseminated elements in them are presented in Table 1.

Dacite of Late Caldera Cycle

The rocks belonging to this period of the Elbrus evolution are exposed in the southwestern part of the volcanic cone (the area of the upper reaches of the Biitik-Tebe and Kyukyurtly rivers). Also referred to this period of time are the dacite and its tuff from the area between the Biitik-Tebe and Kyukyurtly rivers to the Kuban River basin. Also belonging to this period of time are the dacite and its tuff in the area between the Kyrtyk R. and Syltran-Su R. (the latter being a left tributary of the Baksan River). These rocks are restricted to the Syltran magma-feeding fault and compose an erosion monadnock, measuring 8–9 km^2 in area, located 10–12 km ENE of the Elbrus Peak. The left side of the valley in the upper reaches of the Ullu-Kam River shows that a fragment of this rock sequence surrounds the Kyukurtly cone and is cut off by one of the sublatitudinal "caldera-forming" faults. A very important fact is that this fault zone and a fragment of this rock sequence are covered (with angular unconformity) by the Late Neopleistocene dacite lava flows of post-caldera origin. Consequently, the main criteria for classifying these dacite lava flows as an independent late caldera formation cycle are their displacements along the sublatitudinal and submeridional caldera forming faults and their overlapping, with an angular unconformity, by younger dacite lava flows. Similar displacements along submeridional and sublatitudinal caldera-forming faults have been found in this study also at the eastern boundary of the Syltransu volcanic cone. It is important to note that we were the first to discover extrusive bodies in this volcanic cone (Figures 1 and 2). The emplacement of such extrusive bodies usually takes place during caldera formation [*Markhinin,* 1964].

The most complete sequence of the volcanic rocks of the late caldera cycle has been studied in the source area of the Biitik-Tebe River, north of the Biitik-Tebe Glacier. The base of the visible part of the rock sequence is composed of dark gray ignimbrite and light gray rhyolite tuff, referred to the early stage. They are overlain by dark gray and pinkish-gray dacite lavas and lava breccias totaling 200 m in thickness. Above follows a 50–80-meter layer of light gray lava, associated with tuff breccias and lenses of slag-like tuff, forming a "marker level." Exposed further up the section, up to the M. V. Frunze Pass (with an absolute elevation mark of 4050 m), are brownish gray dacite lavas, as thick as 300 m. The precipitous wall hanging over the pass is composed of dark gray banded dacite lava (black at the base) not less than 150 m thick. Outwardly, this part of the rock sequence resembles, in terms of its composition and structure, the Kyzylkol younger and extensive (up to 7 km) lava flow exposed in the upper reaches of the Malka River. Most of the thick lava flows have a three-member structure, the lower and upper layers being usually represented by lava breccias, the intermediate layer being composed of monolithic lava.

The rocks of the late caldera cycle are fairly monotonous in terms of petrography. The most typical is a serial-porphyry microtexture, less common is a glomerophyric microtexture with a pilotaxitic and hyalopilotaxitic groundmass. The middle parts of the thick lava flows have a patchy, micropoikilitic pattern of the groundmass. The common phenocryst minerals are plagioclase, pyroxene, quartz, biotite, and occasional basalt hornblende.

The plagioclase phenocrysts are most variable in terms of morphology. We classified them into several generations included into various associated groups of minerals. For example, the first group of large, first-generation phenocrysts includes tabular, poorly zoned, and often partially fused crystals (1.5–2.5 mm in size) of oligoclase (andesine) containing minute inclusions of biotite, apatite, zircon, and magnetite.

Some of these phenocrysts show a dusty texture. Another variety of large phenocrysts is represented by broad-tabular, complex labradorite crystals, 1.4–2.0 mm in size, and their segregations, 2.5 to 5.0 mm in size, with numerous glass inclusions (skeletal growth). The plagioclase of this variety is often grown over the earlier, more acid variety. The other variety of plagioclase is represented by the elongated crystals (0.1–0.4 mm in size) and microliths of oligoclase-andesine composition.

Pyroxene (hypersthene-bronzite) is found in prismatic crystals, 0.6 to 1.4 mm in size, slightly pleochroic in brownish-pink color.

Biotite is found in scales, 0.5–0.8 mm in size, some of them being unaltered, and most of them being opacitized to a varying degree.

Basaltic hornblende is usually highly opacitized and found in the form of single elongated crystals, 0.5–1.5 mm in size.

The quartz grains, usually smaller than 2.0 mm in size, have a subisometric form and are usually corroded by the groundmass.

The groundmass consists of plagioclase and pyroxene microlites and randomly scattered ore minerals, cemented with glass.

It should be emphasized that dacite contains very small inclusions (less than 1.0–2.0 mm in size) of a holocrystalline rock consisting of rhombic pyroxene, plagioclase, and occasional brown hornblende.

As regards the dating of the igneous activity concerned, it is important to consider the following facts. A continuous outcrop, as long as 500–600 m, in the right side of the Kyukyurty R. Valley, opposite to the glacier of the

Table 2. Contents of petrogenic and trace elements in the lavas of the late post-caldera cycle

Component	Sample number							
	15k-k/97	17R/97	26R/97	21R/97	13k/97	23k/97	15kg/97	19/97
SiO_2	65.4	65.7	65.78	66.5	65.85	66.7	65.85	66.4
TiO_2	0.85	0.78	0.8	0.68	0.76	0.66	0.76	0.86
Al_2O_3	15.45	15.7	15.6	15.6	15.5	15.5	15.7	15.65
Fe_2O_3	1.5	1.87	0.83	1.27	1.45	3.02	1.88	1.2
FeO	2.16	2.55	2.8	2.19	2.53	0.79	2.23	2.75
MnO	0.057	0.058	0.059	0.061	0.06	0.06	0.061	0.057
MgO	1.75	1.81	1.58	2.05	1.78	1.85	2.09	1.77
CaO	3.75	2.75	3.58	2.75	3.02	2.75	2.75	3.3
Na_2O	4.05	3.95	3.99	4.14	4.07	4.04	3.96	3.8
K_2O	3.39	3.4	3.34	3.62	3.47	3.38	3.31	3.21
P_2O_5	0.28	0.3	0.28	0.27	0.29	0.27	0.3	0.3
H_2O	0.24	0.15	0.31	0.1	0.12	0.1	0.17	0.11
CO_2	0.07	0.13	0.07	0.07	0.11	0.13	0.13	0.04
Total	98.947	99.148	99.019	99.301	99.01	99.25	99.191	99.447
Cr	42	45	38	34	42	37	44	63
Ni	36	20	18	33	52	36	18	25
Co	9.7	10	9.2	8	9	7.5	10	11
Sc	8	8.3	8.3	7.3	7	6.9	8	10
Cu	13	9	10	5	11	12	11	10
Pb	12	10	13	12	16	29	12	76
Zn	72	76	84	73	84	74	82	70
W	11.4	2.1	4	1.9	2	1.8	2	2.4
Mo	22.3	12.8	15.8	24.5	15.7	1.7	23.9	34.9
As	5.8	0.7	9	0.6	11.7	8.2	16.3	0.8
Se	0.8	0.8	0.8	0.7	0.7	0.7	2.2	0.9
Sb	0.2	0.2	0.2	0.2	0.1	0.2	0.1	15.4
Ag	2.4	1.7	0.4	1.3	1.7	1.5	1.4	0.5
Rb	134	131	134	145	130	134	119	141
Cs	6.5	6	7.8	6	4.7	6.7	6.2	6
Ba	443	425	595	445	348	405	358	594
Sr	413	393	381	384	415	396	389	387
Ga	25	27	26	21	21	20	28	19
Ta	1.08	1.17	1.23	1.03	0.98	0.93	1.07	1.18
Hf	6.1	6.3	6.7	5.9	5.2	5.4	6.1	7
Zr	349	395	378	338	387	340	398	340
Ti	3638	3798	3600	3310	3646	3302	3987	3698
Y	30	29	17	24	23	25	21	20
Th	21.5	21.5	24.1	21.8	18.9	20.2	19.7	23.5
U	4.7	4.8	5.5	4.8	4	4.2	3.9	5
La	49.5	53.7	53.8	51.2	48.3	46.2	45.6	56.8
Ce	93	96.6	102.9	92.8	85.8	85.2	89.5	96.5
Nd	57	65	56	52	54	47	52	49
Sm	5.65	5.57	6.11	5.28	5.11	4.98	5.35	6.65
Eu	1.28	1.35	1.4	1.23	1.21	1.18	1.31	1.54
Tb	0.6	0.48	0.4	0.45	0.55	0.58	0.63	0.55
Yb	1.6	1.6	1.5	1.2	0.3	1.4	0.3	0.3
Lu	0.2	0.24	0.19	0.16	0.2	0.18	0.21	0.27
F	0.13	0.12	0.11	0.13	0.12	0.13	0.15	0.085

same name, shows dacite lava at the base of the caldera cycle, which overlies successively (from west to east) the Late Paleozoic granites, the Proterozoic mica gneiss, the pumice-ash sequence crowning the early caldera ignimbrite with columnar jointing, and the Late Paleozoic granites again. Consequently, the dacite portion of this sequence accumulated with a significant time break after the formation of pre-caldera explosive rocks, which is proved by the geological evidence from the area between the Kyukyurtli and Ullu-Kam rivers. Here, we discovered dacite lava overlying a light gray loose pumice-ash sequence with a maximum thickness of 8–10 m beyond the boundary of the Elbrus caldera at a relative altitude of 400–450 m above the modern channel of the river. Preserved on the surface of these rocks are moraine remnants consisting of the rounded fragments of the Main Caucasus Ridge rocks and very scarce pebbles of light gray rhyodacite tuff. The Syltran volcanic cone, overlapping the fluvioglacial deposits of Middle Pleistocene age [*Koronovskii,* 1968] and

sitting at a relative height of >350 m above the modern river channel, can be correlated with the dacite of the late caldera formation stage. Thus, the geomorphologic data provide a good enough basis for dating the caldera-stage volcanic rocks Middle Neopleistocene.

Information of the chemical composition of the rocks associated with the caldera-formation stage in the history of the Elbrus volcanic center and of their geochemical specifics is given in Table 2.

Post-Caldera Dacite

Dacite of the Early (pre-Holocene) stage of the Post-caldera cycle. The lava flows composed of the dacite of this stage are widely developed in the upper reaches of the Malka and Baksan rivers, where they are associated with the late (Holocene) volcanics. In the upper reaches of the Baksan River they compose a series of lava flows closely following one another in time and exposed in the area between the Azau and Terskol rivers. In the upper portion of the Malka R. Valley these dacites compose the longest Malka and Kyzylkol lava flows. The Malka lava flow overlaps, without any visible displacement, a series of caldera-forming faults. We found that in the Ullu-Kam–Bolshoi Azau interglacial divide the lava flows of this cycle cover, with an angular unconformity, the dacite of the late stage of the volcano's evolution and are traceable without any displacement above the zone of a sublatitudinal caldera-forming fault. The above evidence provided a good basis for combining the abovementioned lava flows into an independent age group.

The most complete sequence of the volcanic rocks of this stage can be observed in the left side of the glacier part of the Ullu-Kam R. Valley, where it is represented by three lava flows, each of them producing its own independent scarp. The lower flow, as thick as 15–20 m, is composed of dark gray to black glassy dacite with characteristic dark-gray plagioclase phenocrysts showing no distinct crystallographic outlines. Above follows brownish gray, locally thin-plated dacite lava about 50 m thick. This rock sequence is crowned by brown dacite lava 80–100 m thick. Visible between the two upper lava flows are thin lenses of light gray to yellow rocks, obviously tuff, which could not be reached because they occur in the upper part of an almost vertical cliff more than 250 m high. The dacite of the two upper flows contains plagioclase phenocrysts of two generations: the earlier dark gray andesine-labrador crystals (1.5–3.0 mm in size) with indistinct contacts and milky white tabular oligoclase-andesite crystals (2.0–4.0 mm) the cores of which include occasional relics of dark gray andesine (labradorite).

A similar volcanic rock sequence was found in the Garabashi River Valley. Here, an erosion window above the place where a left tributary flows into this river shows the outcrops of dark gray and black dacite lavas with characteristic plagioclase phenocrysts of two generation (dark gray and milky white). These lavas are covered by fluvioglacial deposits almost devoid of any volcanic rock fragments. This rock sequence is overlain by a columnar-jointing lava flow with black glassy dacite exposed at its base. This dacite is overlain by gray dacite with plagioclase and pyroxene phenocrysts. The plagioclase phenocrysts are also represented by two generations similar to those described above. This lava flow is overlain by monotonous brownish dacite lava flows. It is important to note that these lava flows do not contain any independent dark gray plagioclase phenocrysts, this plagioclase occurring merely as relics in the cores of the milky white plagioclase phenocrysts. This rock sequence is obviously incomplete owing to significant breaks in the volcanic activity.

Koronovskii [1968] proposed that the longest Malka (10 km) and Kyzylkol (7 km) lava flows were younger than those from the Azau-Terskol interfluvial area. Yet, the geological solution of this problem is difficult because of their poor exposure and difficult accessibility. An objective solution can be found by isotope or EPR dating using rock-forming quartz. The most representative rocks of this time interval are brownish-gray and dark gray porphyritic lavas with easily distinguishable phases of early crystallization. These lavas are sometimes represented by lenticular, banded (reddish brown and dark gray) and brecciated varieties. In the case of the latter, the fragments of dark gray lava are enclosed in a reddish brown rock mass. The phenocrysts are composed of plagioclase, pyroxene, amphibole, and more occasional biotite and quartz. The rocks have a seriate porphyric microstructure with the hyalomicrolitic and pilotaxitic structure of the groundmass. The groundmass of the rocks is mottled, micropoikilitic in the lava flows of intermediate thickness.

Plagioclase is represented by a gray and a milky white variety. As follows from the results of petrographic studies and microprobe measurements, the gray color of the plagioclase is caused by numerous glass microinclusions. We believe that the presence of this plagioclase in a lava flow can be used as an indirect criterion for correlating rock sequences of a roughly similar age. The plagioclase grains vary greatly in morphology and belong to different generations. The phenocrysts of the first generation include broad tabular labradorite crystals, 1.0–1.5 mm in size, and their concretions (2.0 to 5.0 mm) with indistinct contacts. They also include numerous glass inclusions (skeletal growths). Also common are zoned crystals with idiomorphic edges, where their outer rims do not contain glass inclusions. This plagioclase generation is associated with rhombic pyroxene. There are also some occasional andesine phenocrysts found in association with biotite. They are usually partially fused and overgrown with "skeletal growth" rims with numerous glass inclusions. The microlites of the groundmass (0.01–0.05 mm in size) have an oligoclase composition.

The rhombic pyroxene (hypersthene-bronzite) is found in the form of elongated prismatic crystals 0.3 to 1.0 mm in size and has its inherent optical characteristics. Biotite is developed in the peripheries of the pyroxene grains in the areas of a spotted micropoikilitic structural pattern.

Augite composes crystals, 0.2 to 0.4 mm in size, which display poor pleochroism in brownish colors in some sections.

Basaltic hornblend is opacitized to a fairly great extent.

Biotite relics are found as fragments and opacitized plates.

Quartz is present in the form of scarce subisometric, cor-

Table 3. Contents of petrogenic and trace elements in the lavas of the early post-caldera cycle

Component	Sample number							
	67k/97	56k/97	29k/97	13M/98	44/98	45/98	47/98	57/98
SiO_2	66.85	67.9	66.3	67.25	66.8	66.8	66.4	66.8
TiO_2	0.75	0.72	0.75	0.75	0.7	0.8	0.75	0.7
Al_2O_3	15.57	14.6	14.7	14.9	15	15	15.25	15.85
Fe_2O_3	1.17	1.22	0.99	1.72	1.21	1.15	1.46	1.67
FeO	2.13	2.37	3.07	2.32	3.04	2.83	3	1.65
MnO	0.06	0.054	0.067	0.088	0.078	0.075	0.072	0.049
MgO	1.38	1.43	2.06	1.97	1.33	1.4	1.45	0.85
CaO	3.48	2.86	3.13	2.09	2.96	3.11	3.22	2.2
Na_2O	4.05	3.92	3.91	3.97	4.13	4.23	4.2	3.73
K_2O	3.69	3.42	3.22	3.64	3.3	3.47	3.4	3.39
P_2O_5	0.26	0.23	0.25	0.23	0.3	0.3	0.25	0.22
H_2O	0.15	0.1	0.1	0.05	0.11	0.17	0.27	0.22
CO_2	0.07	0.04	0.07	0	0.22	0.07	0.22	0.11
Total	99.61	98.864	98.617	98.978	99.178	99.405	99.942	97.439
Cr	32	0	39	31	42	39	33	40
Ni	29	13	26	20	33	23	25	18
Co	6.5	0	9	8.7	11.6	10.4	10.4	6.4
Sc	6.5	0	8	8	8.7	9	8.2	8.5
Cu	5	7	5	8	13	9	8	8
Pb	10	130	5793	12	12	12	10	11
Zn	58	73	335	53	64	63	59	56
W	2.1	0	4.4	0.8	0.6	0.6	0.6	0.9
Mo	15.9	0	8.5	10.4	7.2	8.7	10.3	9.8
As	0.7	5	2.2	9.3	8.5	8.5	7.6	10.1
Se	0.8	0	3	2	0.6	0.6	1.6	0.5
Sb	0.2	0	1048.7	0.4	0.3	0.4	0.05	0.5
Ag	0.4	0	7.7	0	0	0	0	0
Rb	152	170	170	149	139	137	139	160
Cs	6.3	0	0.3	8.5	10	9.8	10.6	17.6
Ba	440	0	164	507	500	109	539	612
Sr	416	315	370	343	361	368	372	275
Ga	22	20	9	15	17	16	15	17
Ta	0.86	0	0.5	1.02	1.12	1.18	1.13	1.27
Hf	5.1	0	4.8	5.4	6.3	6.3	6	6.4
Zr	364	300	2286	148	196	200	177	165
Ti	3058	3000	3626	3112	3772	3528	3347	2994
Y	20	26	10	13	13	14	10	13
Th	20.5	0	21.3	23.9	25.6	26	27.2	26.5
U	5	0	1.4	3.2	4.9	5	4.9	5.8
La	42.2	0	44.2	52	49.6	51.1	50.4	51.7
Ce	72.3	0	76.3	81.9	90.6	92.8	89.9	81.2
Nd	35	0	34	38	40	46	42	42
Sm	4.56	0	5.53	5.49	5.55	6.8	6.42	5.89
Eu	1.1	0	0.97	1.12	1.29	1.39	1.29	1.16
Tb	0.44	0	0	0.41	0.74	0.76	0.65	1.44
Yb	1.4	0	0.4	1.3	1.9	1.7	1.3	1.7
Lu	0.14	0	0.05	0.17	0.19	0.18	0.16	0.18
F	0.11	0.083	0.081	0.05	0.075	0.073	0.08	0.075

roded crystals (0.5 to 1.0 mm in size), often surrounded by reaction rims ("pyroxene coronas") which prove its xenogeneous origin.

Before substantiating the age of this rock sequence, it should be noted that in the left side of the Azau R. Valley the basal parts of the tree lava flows of the early caldera formation cycle rest at the relative elevations of 150, 200, and 250 m, respectively, in the manner similar to that of the Malka lava flow (100–200 m), above the present-day river channel. Moreover, these lava flows overlie a moraine which has been dated 22–24 thousand years, using geomorphologic data, this providing a basis for dating their lower age limit. Their upper age limit is controlled by the fact that all lava flows show the evidence of denudation topographic elements produced during the end of the late Neopleistocene glaciation.

Late (Holocene) dacite. The lavas of this cycle cover in a mantle form all of the older volcanic rocks. The area of their extent coincides fairly closely with the Late Neopleistocene lava flows with some displacement eastward. They also compose both of the Elbrus summit craters. The most extensive lava flows occur in the drainage area of the Birdzhali-Su R. basin (source of the Malka River) and in the area between the Azau and Terskol rivers (Baksan R. source). Most of the Holocene lava flows descend steeply into the river valleys and show a blocky (aa-lava) surface. It should be noted that in addition to volcanic activity, that period of time was marked by a significant explosive activity. An example is a subhorizontal rock sequence, 60–80 m thick, exposed in fragments at the base of the eastern summit crater, on its southeastern side, near the saddle. It consists of light gray porous rocks of a complex origin, which include clastic pumice tuff. In our opinion, this horizon can be used as a marker for the Holocene volcanic rocks and, as follows from its geologic position, had been associated with the explosive activity in the crater of the western peak. It is important to mention that this horizon can be traced visually also in the area southwest of the western peak, where the same rock material composes a gentle water-divide area with elevation marks of 4880–4900 m. The ash and pumice lenses, synchronous with this layer, have been found far from the Elbrus Mt. in the low terraces of the Baksan and Chegem rivers.

All of the studied lava flows are composed of monotonous black glassy dacite lava with clearly visible phases of early crystallization. Most of the phenocrysts are composed of plagioclase with significantly less numerous dark-color minerals (amphibole, pyroxene, and biotite) and quartz. The rocks have a serially porphyritic texture and a hyalopilotaxitic groundmass consisting of plagioclase microlites, oriented more or less in the same direction, and randomly scattered hornblende and pyroxene grains.

Plagioclase (andesine) occurs in broad tabular, occasionally corroded crystals (0.7–1.5 mm in size) and their growths (2.0–3.0 mm in size), associated with biotite. There is also a second plagioclase generation with crystals ranging from 0.05–0.3 to 0.15–0.5 mm in size, which corresponds to labradorite in composition, these crystals containing numerous glass inclusions. This plagioclase generation is associated with pyroxene and very rarely with hornblende. The quantitative relationships of these generations vary substantially from one lava flow to another.

Orthopyroxene (bronzite) is found in prismatic crystals smaller than 0.15–0.4 mm in size.

Basaltic hornblende occurs in the form of fresh (unaltered) crystals or of crystals with operatic rims, less than 0.5–1.0 mm in size.

Biotite plates, 0.3 to 0.5 mm in size, are usually opacitized to various degrees.

Quartz is distributed extremely irregularly in the rock and is found in the form of subisometric corroded crystals, 0.5 to 4.0 mm in size, occasionally enclosed in clinopyroxene rims.

The lower age limit for the volcanic stage concerned is the last phase of the Late Pleistocene glaciation, the early Holocene lava flows being embedded in the elements of the exaration topography [*Koronovskii,* 1968]. Three lava flow generations of different ages have been mapped in the Holocene rock sequence and, proceeding from their relations with the historical glacial deposits and those emplaced during the 19th century, it was assumed that the lava flows emplaced during the latest Elbrus eruptions must be dated 2.0–1.5 thousand years [*Koronovskii and Rudakov,* 1962].

Proceeding from the results of the radiocarbon dating of humusized buried soil and of old coals enclosed in them, it was found [*Bogatikov et al.,* 1998a, 1998b] that during the Holocene the volcanic activity of Elbrus was repeated several times, namely, 6250±50, 4270±40, 1330±80, and 99±60 years ago. It is obvious that far from all Holocene eruptions have been dated thus far.

The chemical compositions of the rocks emplaced during the post-caldera Late Pleistocene and Holocene periods of the Elbrus evolution and their geochemistry are presented in Tables 3 and 4.

Specific Petrochemistry and Geochemistry of Elbrus Volcanic Rocks

During our comprehensive study of the Elbrus Volcano we created a database (>660 analyses), including the results of the neutron activation, X-ray fluorescence, and classical chemical analyses of rocks and some rock-forming minerals, grouped into individual data samples. Our data samples chosen from the numerous analytical determinations of some elements include geochemical data that characterize the volcanic rocks of all chosen stages and cycles in the evolution of the Elbrus volcanic center. The geochemistry of the rocks is presented in Tables 1 to 4.

This paper was not intended to trace the behavior of the contents of individual elements in the rocks, characterizing the successive periods and cycles in the Elbrus volcanic evolution. Our purpose was to distinguish some general geochemical features characteristic only of the Elbrus Volcano, which could be compared with any other volcanic centers.

For this purpose we used the idea of the element formula proposed by *Kozlov et al.* [1977] with some of our own additions. This element formula characterizes the extent of the anomalous character of the elements in particular types of the volcanic rocks, expressed in clarke portions.

The numerator of the formula is used for accumulating elements, and the denominator for disseminated elements with concentrations below the clarke values. Elements with concentrations close to the clarke values (0.8–1.5) were discarded. In view of the fact the volcanic rocks concerned had a dacite composition, the formulas were calculated using the clarkes for acid rocks after *Vinogradov* [1962]. The method of three sigmas was used to discard "hurricane" values, that is, the values higher than the module of a mean value by the value of a threefold standard deviation were discarded.

Given below are the element formulas for the Elbrus volcanic rocks.

1. Ignimbrites and the associated tuffs of the early caldera cycle (89 samples): Ag (35.9), Se (29.7), Mo (14.2), As (5.7), Hf (5.4), Sb (3.2), Cs (2.9), Ni (2.3), Sc (2.2), U (2.0),

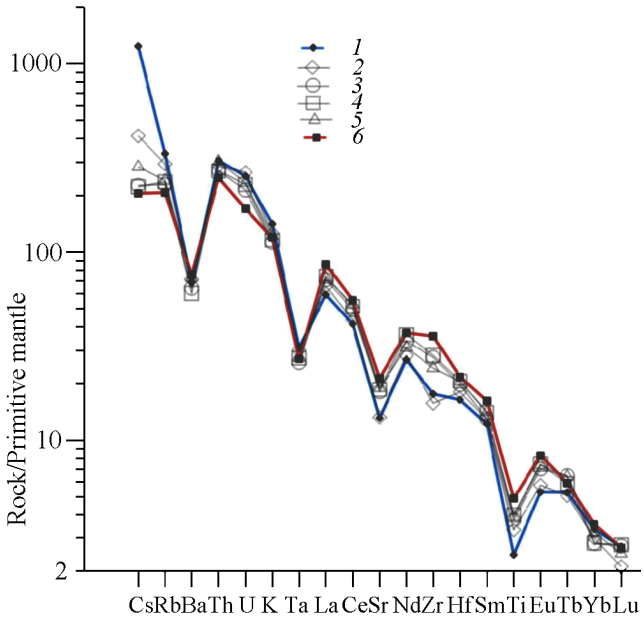

Figure 5. Spider diagram for the Elbrus volcanic rocks. The composition of the primitive mantle is given after [*Sun and McDonough,* 1989].
Legend: (1) precaldera stage (Late Pliocene); (2) rhyodacite of the early caldera cycle (Early Neopleistocene); (3) dacite of late caldera-formation cycle; (4) dacite of early post-caldera cycle; (5) dacite and trachydacite of late (Holocene) post-caldera cycle; (6) trachyandesite of the Tash-Tebe erosion outlier (Late Neopleistocene) of the early post-caldera cycle.

Co (1.3), Cr (1.2), Lu (0.2), Tb (0.3), Ta (0.4), Yb (0.4), Cu (0.4), Y (0.5), Ba (0.5), Sm (0.6), and Eu (0.7).

2. Dacite of the late caldera cycle (238 samples): Ag (32.2), Se (20.6), Mo (12.6), Hf (6.2), As (3.5), Sb (3.5), Ni (3.2), Sc (2.7), Cs (2.3), Co (1.7), Cr (1.6), Zr (1.6), Lu (0.2), Tb (0.3), Ta (0.3), Yb (0.3), Cu (0.5), Y (0.5), Ba (0.6), Sm (0.7), and Rb (0.7).

3. Dacite of the early post-caldera cycle (154 samples): Ag (33.7), Se (23.5), Mo (15.3), Hf (5.8), Sb (4), As (3.7), Ni (3.3), Sc (2.6), Co (1.8), Cr (1.7), Zr (1.7), W (1.7), Lu (0.2), Tb (0.2), Ta (0.3), Yb (0.3), Cu (0.4), Y (0.5), Ba (0.6), Sm (0.6), and Rb (0.7).

4. Dacite of the late (Holocene) stage of the caldera formation cycle (173 samples): Ag (34.5), Se (21.7), Mo (13.9), Hf (5.7), Sb (5.7), Ni (3.3), As (3.1), Sc (2.7), Co (2.0), Cr (1.8), Cs (1.6), Lu (0.2), Tb (0.3), Ta (0.3), Yb (0.4), Y (0.4), Cu (0.5), Df (0.6), Sm (0.6), Rb (0.7).

5. Elbrus airborne ash (early post-caldera cycle) from the area of the Temirzhbek Village (8 samples, Ag was not determined): Se (10.6), Mo (10.0), As (9.4), Hf (6.1), Sb (5.8), Ni (3.2), Sc (2.0), Th (2.0), U (1.6), Lu (0.2), Ta (0.5), Yb (0.5), Y (0.5), W (0.6), Cu (0.6), Cr (0.7), Eu (0.7).

These geochemical formulas show that the rocks of all stages of the Elbrus volcanic center evolution show the same assemblages of chemical elements both in the numerators and in the denominators of the formulas. It is important to note that the sequence order remains fairly the same. Some differences can be found only in the cases where the contents of some elements approach the clarke values.

The analysis of the formulas shows that the volcanic rocks of all successive stages of the Elbrus center evolution show high Ag, Se, Mo, Hf, As, and Sb contents and also elevated Ni, Sc, Cs, Co, and Cr concentrations. At the same time all rocks are poor in Lu, Tb, Ta, Yb, Y, Cu, Ba, Sm, Eu, and Rb. In our opinion these geochemical features are typical of the volcanic rocks of the Elbrus Center. To verify this supposition, we computed the analytical data for three samples of ash which had been transported by air over a distance of 285 km from Elbrus to the Temirzhbek Village. The same elements (except Ag) were determined in the ash. Some differences in the behavior of W and, especially, of Cr, seem to have been associated with the small number of samples analyzed, this, in turn, increasing the possibility of random errors.

The similar petrochemical and geochemical compositions of the whole evolution series of the Elbrus volcanic rocks seem to suggest the stable thermodynamic conditions of the rock melting at the level of a magma chamber. At the same time the analysis of the above formulas shows that the contents of Sb, Ni, Cr, and Co increase gradually and that of Cs declines.

The examination of the data presented in Tables 1 to 4 shows that the effusive, explosive, and extrusive rocks developed in the earthquake focal zone of the Main Caucasus Ridge show a similar petrochemical composition corresponding to rhyodacite, dacite, and less frequently to trachydacite. The main petrochemical features and geochemical parameters of all rocks examined are close to those of type-I orogenic granitoids [*Chappell and White,* 1974; *Frost et al.,* 2001; *Rozen and Fedorovskii,* 2001]. As mentioned above, the more basic volcanic rocks are present only in the north of the Elbrus region, in the Bechasy and Frontal Range focal zones, a few dozens of kilometers from Elbrus, having mainly a trachyandesite or less commonly a basaltic andesite composition. Most of the volcanic rocks are exposed in the earthquake focal zone of the Main Ridge, in the area of the long-lived Elbrus volcanic center (EVC), where we distinguished caldera and post-caldera cycles with early and late periods. Generally, the EVC volcanic rocks (rhyodacite, dacite, and trachydacite) show high alkali contents (totaling 6.83–8.15%) and fairly high K_2O/Na_2O values, which make them similar to potassic subalkalic rocks.

The spider diagram presented in Figure 5, where the concentrations of chemical elements are normalized to the composition of the primitive mantle, shows that all volcanic rocks of the Elbrus volcanic region show, irrespective of their compositions, small negative Ba, Sr, Ta, and Ti anomalies, this proving them to be geochemically similar.

The gray lines in Figure 5 show the average compositions of the volcanic rocks of the caldera and post-caldera cycles, the gray lines showing the pre-caldera rhyodacite (Late Pliocene) and the trachyandesite of the Tash-Tebe Volcano (Late Neopleistocene). Proceeding from the compositions of the melt inclusions in the phenocryst minerals of the Elbrus

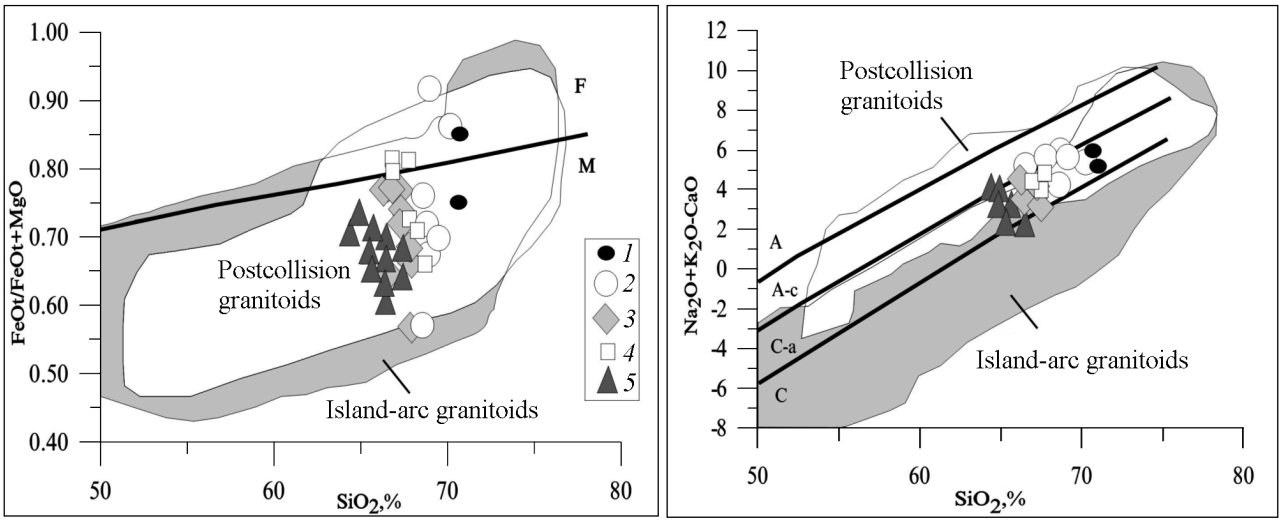

Figure 6. The positions of the Elbrus volcanics in classification diagrams, after *Frost et al.* [2001]. Legend: granitoids: (F) ferrous, (M) magnesian, (C) calcareous, (C-a) calcareous-alkaline, (A-c) subalkalic, (A) alkalic; (1, 2) rhyodacite: (1) precaldera), (2) early-caldera; (3–5) dacite: (3) late-caldera cycle, (4) early post-caldera cycle, (5) late (Holocene) post-caldera cycle.

volcanic center, the two latter varieties of the rocks might have been independent phases, the mixing of which produced dacite melt. Figure 5 shows that the distribution of trace elements in the Elbrus dacite is similar to that observed in the pre-caldera rhyodacite and trachyandesite, their contents being intermediate between those in the final members. Our least-square calculations showed that the amount of acid melt must have been as great as 80% for the formation of hybrid dacite melt, during the mixing of rhyodacite and trachyandesite magmas and during the formation the rhyodacite of the early caldera formation cycle; this value must be 39% for the formation of early-caldera dacite, 39% for the dacite of the early caldera formation cycle, 38% for the early post-caldera cycle, and 32% for the late post-caldera cycle.

Note that the hybrid dacite produced by the mixing of rhyolite and andesite melts is widely developed in the Miocene rock sequence in the Transcarpathian region [*Lazarenko and Deichakovskaya,* 1973]. These rocks originated under similar geologic conditions in the region between the Pannonian Massif, where acid volcanic rocks were erupted, and the Transcarpathian internal basin, where huge volcanic eruptions produced mainly intermediate rocks. However, the Elbrus volcanic center is known for the more perfect homogenization of its hybrid magmas.

In the $FeO_{tot}/FeO_{tot}+MgO$) – SiO_2 and (Na_2O+K_2O-CaO) – SiO_2 diagrams (Figure 6), the data points are plotted in the area of the convergence of the fields of island-arc and post-collision granitoids. This suggests their transitional position from the collision to the post-collision rocks.

Important evolution information can be obtained from the distribution pattern of the petrochemical data in the successive stratigraphic rock sequence of the stratovolcano. The SiO_2 contents in the pre- to post-caldera rocks of the volcanic center concerned vary from 70.5 to 64% (Figure 7). Higher silica contents were found in the ignimbrites and lavas of the pre-caldera and early caldera cycles, where they vary from 66 to 70.5%, whereas in the later volcanic rocks these values are in the range of 65–67.5%, and only in the lavas of the Eastern Peak the SiO_2 content declines to 64.2%. Consequently, the observed SiO_2 variation has a poorly expressed antidrome trend.

Figure 7 shows that there is some correlation between the contents of petrogenic elements and silica in the volcanic rocks of all cycles recognized in the Elbrus volcanic area. As the SiO_2 contents decline, the volcanic rocks grow higher in TiO_2, FeO, MgO, CaO, and P_2O_5, and lower in K_2O. The Elbrus volcanic rocks show a clearly expressed change in the contents of Na_2O and Al_2O_3 with a change in the SiO_2 contents. Note that a similar pattern of correlation among the petrogenic elements has been obtained from the melts of ore materials in the rock-forming minerals of the Elbrus volcanic region (Figure 5).

The comparison of the relative roles of K and Na in the acid rocks (mainly in feldspar), using I. V. Nosyrev's method [*Belyaev and Rudnik,* 1978], represented graphically in the N and K coordinates (at. %), where $N=N_2O/[(Al_2O_3+Fe_2O_3) – (K_2O+CaO)]$ and $K=K_2O/[(Al_2O_3+Fe_2O_3)-(Na_2O+CaO)]$, showed (Figure 8) that the data points of the volcanic rocks resided in the region of N>K and occasionally on the N=K line. The line of equal N and K values corresponds to the acid rocks, whose Al_2O_3, CaO, Na_2O, and K_2O components showed eutectic relations, the 100% of the eutectic mixture being marked by a point with N=K=1 coordinates. The compositions of the Elbrus rocks (from the caldera to the post-caldera cycle) move successively toward the N coordinate. This points to the growth of the relative Na role in the melt in the course of its evolution.

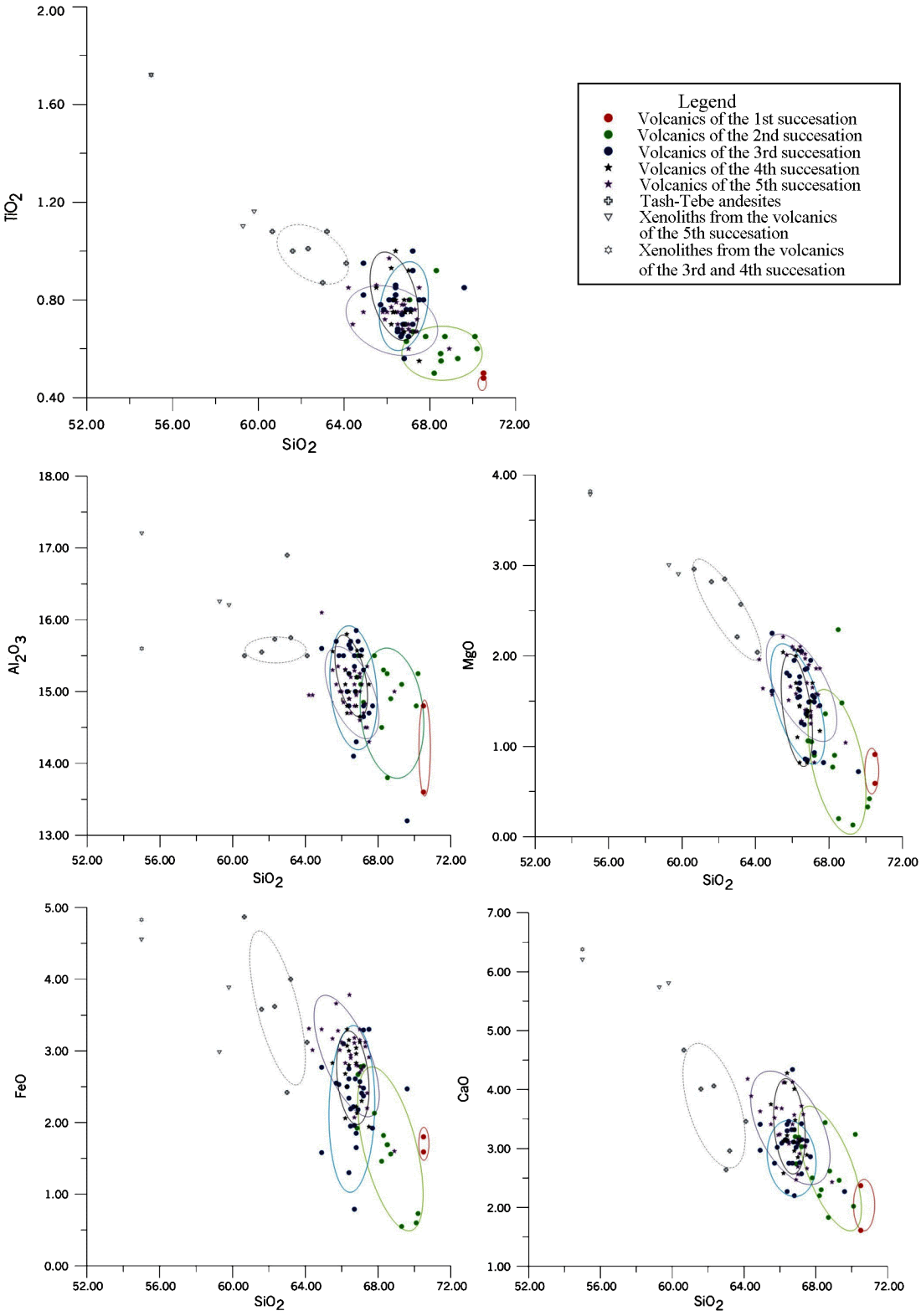
Legend
Volcanics of the 1st succesation
Volcanics of the 2nd succesation
Volcanics of the 3rd succesation
Volcanics of the 4th succesation
Volcanics of the 5th succesation
Tash-Tebe andesites
Xenoliths from the volcanics of the 5th succesation
Xenolithes from the volcanics of the 3rd and 4th succesation
TiO2
Al2O3
MgO
FeO
CaO
SiO2
52.00
56.00
60.00
64.00
68.00
72.00

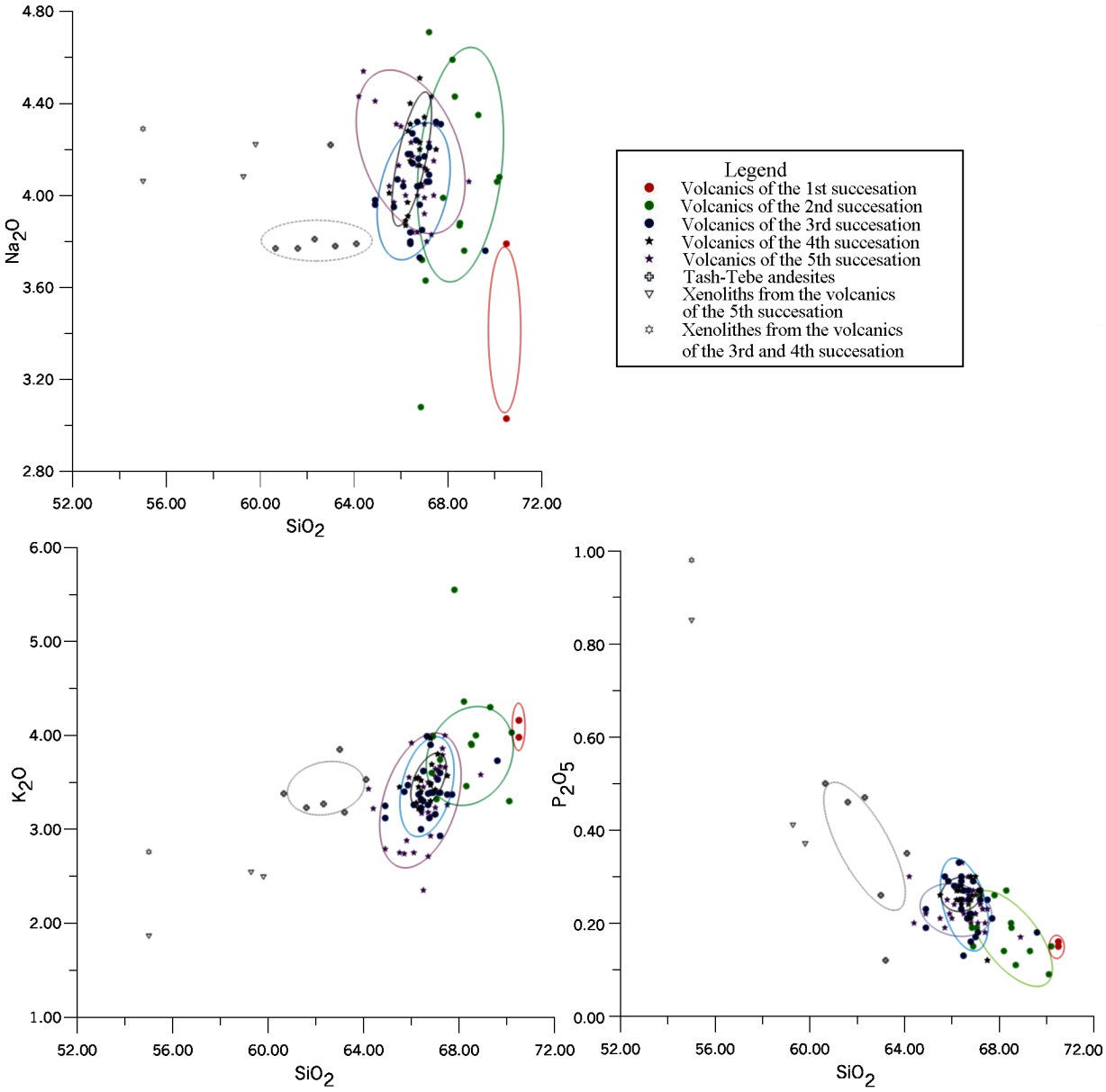

Figure 7. Variation diagrams of SiO_2 – petrogenic elements for the volcanics of the Elbrus region. Legend: Volcanics of the 1st succesation, Volcanics of the 2nd succesation, Volcanics of the 3rd succesation, Volcanics of the 4th succesation, Volcanics of the 5th succesation; Tash-Tebe andesites; Xenoliths from the volcanics of the 5th succesation; Xenolithes from the volcanics of the 3rd and 4th succesation.

Table 4. Contents of petrogenic and trace elements in the lavas of the late (Holocene) post-caldera cycle

Component	Sample number								
	58k/97	33Ka-11/97	38K/97	34kb/97	28K/97	8/98	10/98	44/98	48/98
SiO_2	65.85	65.5	66.8	66.7	65.7	65.8	64	66.8	67
TiO_2	0.79	0.86	0.78	0.78	0.78	0.75	0.75	0.7	0.7
Al_2O_3	14.9	15.3	14.95	15	15.1	15.25	16.1	15	14.6
Fe_2O_3	0.61	1.52	1.44	0.47	0.78	1.16	0.98	1.21	0.8
FeO	3.78	3.14	2.8	3.18	3.66	3.28	3.3	3.04	3.15
MnO	0.07	0.07	0.06	0.071	0.072	0.081	0.085	0.078	0.072
MgO	2.1	2.21	1.7	2.02	2.01	1.51	1.57	1.33	1.39
CaO	3.3	3.41	3.57	3.41	3.52	3.69	3.63	2.96	3.16
Na_2O	4.23	4.04	4.04	4	3.97	4.31	4.41	4.13	3.99
K_2O	3.17	2.75	2.93	2.71	2.74	2.88	2.79	3.3	3.56
P_2O_5	0.33	0.21	0.2	0.3	0.19	0.25	0.22	0.3	0.22
H_2O	0.13	0.1	0.1	0.1	0.1	0.22	0.26	0.11	0.31
CO_2	0.09	0.07	0.04	0.15	0.04	0.15	0.22	0.22	0.11
Total	99.35	99.18	99.41	98.891	98.662	99.331	98.315	99.178	99.062
Cr	49	43	39	49	59	50	47	42	47
Ni	48	17	15	19	25	20	63	33	29
Co	9.7	9.7	8	9	12	11.4	11.7	11.6	11
Sc	8.6	8.5	7	8	10	8.9	9.4	8.7	8.4
Cu	10	9	8	7	6	16	4	13	12
Pb	29	372	40	136	4987	10	8	12	10
Zn	73	87	69	78	243	63	53	64	62
W	2.5	2	1.7	1.9	5	1	1	0.6	0.6
Mo	20.1	2	17.4	12.7	8.3	8.5	6.9	7.2	10.5
As	7.2	0.7	0.5	0.6	2.2	5.8	5.8	8.5	6.7
Se	0.9	0.9	0.7	0.8	3	0.6	0.6	0.6	0.6
Sb	0.2	64.5	4.2	20.4	983.2	1.7	0.05	0.3	0.2
Ag	2.1	1.3	1.3	1.7	7.8	0	0	0	0
Rb	123	124	138	130	138	110	90	139	145
Cs	6.5	5	7.7	5.4	0.3	7	7.2	10	10.2
Ba	346	379	358	409	163	406	428	500	513
Sr	444	385	356	347	366	369	335	361	314
Ga	20	16	22	20	7	17	10	17	18
Ta	0.97	0.95	0.91	0.84	0.49	0.82	0.79	1.12	1.06
Hf	5.7	5.2	5.4	5.9	6.1	5.8	5.2	6.3	6.2
Zr	397	324	318	337	339	188	128	196	169
Ti	3735	3984	3559	3806	4053	3478	2622	3772	3183
Y	19	20	19	22	10	12	8	13	13
Th	18.7	18.4	19.5	19.4	20.1	20.3	18.9	25.6	28.4
U	3.6	4.9	4.4	3.9	1.4	3.1	3.4	4.9	5
La	45.8	42.7	42.5	44.7	47.9	44.8	40.3	49.6	51.5
Ce	77.7	78.3	78.4	80.9	79.3	78.6	68.5	90.6	92.4
Nd	35	47	42	9	34	40	35	40	42
Sm	5.37	4.82	4.86	5.11	5.28	5.48	5.07	5.55	6.37
Eu	1.25	1.22	1.11	1.14	1.31	1.19	1.15	1.29	1.19
Tb	0.57	0.48	0.82	0.63	0.59	0.67	0.88	0.74	0.72
Yb	1.4	1.5	1.3	0.3	0.4	1.5	1.5	1.9	1.4
Lu	0.21	0.18	0.15	0.19	0.05	0.17	0.2	0.19	0.1
F	0.12	0.07	0.074	0.071	0.09	0.063	0.064	0.075	0.054

Compositions of Elbrus Lavas From the Study of Melt Inclusions in Phenocryst Minerals from the Elbrus Volcanic Center

In spite of the numerous papers describing the geological structure, magmatism, petrography and mineralogy of the Elbrus and Kazbek volcanoes [*Bogatikov et al.,* 1998a, 1998b; *Koronovskii,* 1968; *Masurenkov,* 1961; *Popov,* 1981; *Stankevich,* 1976], to name but a few, some problems related to the origin and evolution of the magmas still remain to be poorly studied.

Before discussing the petrogenesis of the magmas that had produced the Elbrus Cone, it should be noted that we found abundant xenoliths (inclusions) of intermediate and basic rocks (basaltic andesite) ranging from fractions of a centimeter to a few dozens of the latter in size in the dacite lavas. Moreover, these rocks include ubiquitous quartz xenocrysts with pyroxene coronas and those of basic plagioclase, overgrown with a more acid rim, and also those of basic plagioclase with more acid rims. Proceeding from these finds, we assumed that two melts had mixed in the course of the eruption, namely, a crustal rhyodacite melt and a deeper melt of basaltic andesite. This assumption, based on geologic and petrographic evidence, was later confirmed by our Sr and Nd isotope studies in different rock types. For instance, the outliers of precaldera trachyandesite (mouth of the Khudes R.) and of trachybasaltic andesite (upper reaches of the Tyzyl R.) [*Chernyshev et al.,* 2001; *Ivanov et al.,* 1993] showed the $^{87}Sr/^{86}Sr$ values to be 0.706143 and 0.705091–0.705196, and the $^{143}Nd/^{144}Nd$ values, expressed in ε_{Nd}, to vary from −0.94 to −1.23. As to the post-caldera dacites from different lava flows of the Elbrus Volcano and found in basaltic andesite xenoliths, the Sr ratios vary from 0.70525 to 0.706533 and from 0.705265 to 0.705386, the ε_{Nd} values varying from −1.32 to −1.95 and from −0.33 to −0.86, respectively.

The isotope data presented above prove fairly convincingly the notable role of the mantle component in the melts that produced the Elbrus volcanic center. It appears that these magmas had originated from the mixing of basalt or basaltic andesite melts, derived from some mantle source, with an acid (rhyodacite) crustal melt. Another possible mechanism is the contamination of the crustal acid magma by some basic magma having an indirect mantle origin.

In order to confirm or refute this supposition, we carried out a special-purpose study of the compositions of melt inclusions in phenocryst minerals and in the groundmass and determined the temperature of their homogenization. In the case of the mixing of two melts differing in composition and depth we were supposed to get two compositionally different types of melt inclusions. In this case the rhyolite and dacite inclusions must have been superheated.

We studied melt inclusions in plagioclase and quartz phenocrysts from the rocks of some lava flows and their intermediate to basic xenoliths, and also from the ignimbrites of the Elbrus Volcano. We used the methods of the homogenization of these inclusions and the analysis of their glasses (more than 30 determinations), and of the groundmass glasses (17 determinations) using an electronic microprobe.

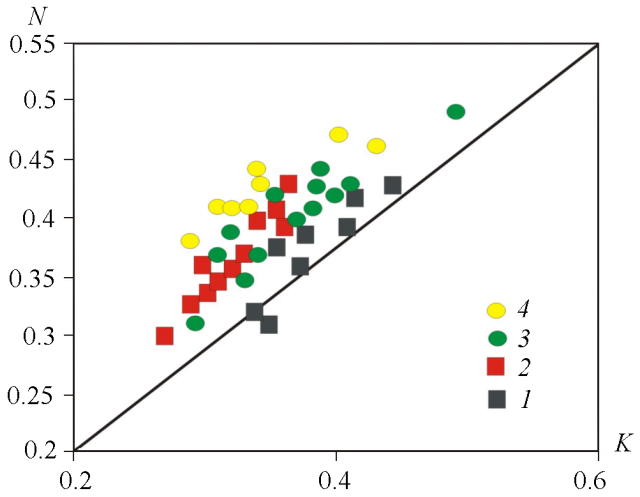

Figure 8. Positions of the Elbrus volcanics in the I. V. Nosyrev's diagram.
Note. $N=Na_2O/[(Al_2O_3+Fe_2O_3)-(K_2O+CaO)]$, $K=K_2O/[(Al_2O_3+Fe_2O_3)-(Na_2O=CaO)]$. The line of equal N and K values corresponds to the acid rocks whose Al_2O_3, CaO, Na_2O, and K_2O components have eutectic relations, the point with the coordinates of N=K=1 marking a hundred percent eutectic mixture. (1) precaldera and early caldera rhyodacite; (2–4) dacite: (2) dacite of late caldera formation time; (3) dacite of early caldera formation time; (4) dacite of late (Holocene) post-caldera formation cycle.

It should be noted that some scarce analyses of primary melt inclusions, in particular those of rhyolite with high K_2O contents (4.5 to 6.1 wt %), found in quartz phenocrysts (Malka lava flow) and in plagioclase phenocrysts (Azau lava flow), were made [*Popov,* 1981]. Melt inclusions were also analyzed in the minerals from the Elbrus rocks [*Babanskii et al.,* 1995; *Naumov et al.,* 1990]. The latter researchers found that the inclusions in plagioclase and quartz from dacitic andesite, dacite, and rhyodacite had been homogenized at high temperatures (>1100°C), had a composition similar to that of rhyolite with the predominance of K over Na, and were low in volatiles (H_2O, Cl, F).

The aim of our research was to study systematically the melt inclusions in the successively emplaced lava flows composing the Elbrus Cone and some small subsidiary volcanic centers (Tash-Tebe and Syltra)in the vicinity of Elbrus.

Geological description of the study objects. As follows from the latest data, Elbrus Volcano is a derivative of some long-lived magma system that originated in the western limit of a collision structure controlled by a system of deep submeridional faults. The Elbrus volcanic cone (the absolute elevations of its foundation being 3200–3400 m) is a horizontally isometric, polygenic stratovolcano, the formation history of which included several cycles of volcanic activity from different, though closely spaced volcanic cones, namely, the western and eastern cones of Elbrus and a re-

Table 5. Location of the samples

Sample no.	Sample rock	Sampling area
25/97	Ignimbrite	Elbrus Volcano, source of Biitik-Tebe R.
34/97	Dacite lava flow	Syltran volcanic cone in Elbrus area, Syltran-Su R.
36/97	–	–
44/97	–	Elbrus Volcano, Malka lava flow, Malka R. source area
45/97	–	Elbrus area, Malka R. source (Zhila-su Holocene lava flow)
47/97	Ignimbrite	Elbrus Volcano, source of Malka R. area (Aerodrom site)
50/97	Andesite lava flow	Elbrus area, Tash-Tebe small shield volcano in the left side of the Tokhana-Su R. Valley.

cently discovered and mapped fragment of the Kyukyurtly volcanic cone. Most of the Elbrus lava flows are composed of dacite and occasional rhyodacite of a high-K calcareous-alkaline series. The Tash-Tebe and Syltran small independent volcanoes, having the same magma source as the Elbrus Volcano, are located northwest and northeast of the latter.

Description of rock samples. For the purpose of studying melt inclusions samples of the most typical rocks were collected from the lava flows of different ages and from the tuff beds of the caldera and post-caldera cycles of the Elbrus activity: dacite, dacitic andesite, and rhyodacite tuff and ignimbrite. In the Elbrus volcanic history, ignimbrite had been associated with the earliest phase of the Elbrus evolution, namely with the formation of a caldera. Samples of these rocks have been collected in the valleys of the Biitik-Tebe and Malka rivers (Table 5). These are pinkish-gray massive, occasionally fluidal, rocks containing quartz, plagioclase, and biotite phenocrysts. Their distinctive feature is the presence of fiamme.

The dacite marks the early and late periods of the Elbrus caldera and post-caldera volcanic activity. The samples of these rocks were collected in the valleys of the Malka and Biitik-Tebe rivers and in the Tash-Tebe small single-act volcano (Table 5).

Outwardly these are dark gray to black massive, occasionally porous, obviously porphyritic rocks. Their phenocrysts are composed mainly of plagioclase and of less common pyroxene, hornblende, and quartz.

We also studied the samples of dacite lava from the Syltran and Tash-Tebe volcanic cones (samples 36/97 and 50/97, respectively) located NE and NW of Elbrus. Dacite has a porphyry structure with phenocrysts usually composed of plagioclase and less commonly of pyroxene, biotite, and quartz. The distinctive feature of these rocks is the presence of numerous melanocratic inclusions composed of a plagioclase-pyroxene aggregate.

The chemical compositions of the Elbrus rocks used to study melt inclusions are presented in Table 6, the representative analyses of their plagioclase phenocrysts are given in Table 7.

Studies of magmatic inclusions in minerals. The minerals from the studied samples were found to contain crystalline (usually accessory) minerals and melt inclusions. The latter were studied in plagioclase and quartz. No fluid inclusions have been found so far. Remind that most of the phenocrysts in all Elbrus rocks are dominated by pla-

Table 6. Chemical compositions (wt %) of the Elbrus rocks, the phenocrysts of which were used to study melt inclusions

Component	Sample number						
	50/97	45/97	44/97	25/97	34/97	36/97	47/97
SiO_2	63.20	66.28	66.65	67.56	67.89	68.81	70.92
TiO_2	1.08	0.75	0.68	0.60	0.77	0.63	0.44
Al_2O_3	15.75	15.80	15.55	14.77	15.67	15.11	15.01
FeO	6.06	3.45	3.74	3.68	3.40	3.69	2.72
MnO	0.07	0.06	0.07	0.06	0.06	0.06	0.05
MgO	2.57	1.10	1.38	1.11	1.50	1.26	0.79
CaO	2.69	4.12	2.89	2.58	3.12	2.89	1.73
Na_2O	3.78	3.97	3.76	3.95	3.11	3.43	3.57
K_2O	3.18	3.55	3.28	3.42	3.44	3.77	3.84
P_2O_5	0.12	0.28	0.23	0.16	0.25	0.19	0.11
LOI	1.06	0.47	n.d.	1.89	0.58	0.50	0.87
Total	99.56	99.83	98.23	99.78	99.79	100.34	100.05

FeO denotes total iron, n.d. – not determined.

Table 7. Representative compositions (wt %) of plagioclase phenocrysts from the studied rocks of the Elbrus Volcano

Component	Sample number						
	25/97	50/97	44/97	25/97	45/97	45/97	34/97
SiO_2	54.15	53.48	52.58	59.14	60.11	61.42	60.24
Al_2O_3	27.31	29.48	30.01	25.07	23.05	22.54	24.62
CaO	11.59	10.94	10.49	7.52	6.45	5.59	5.44
Na_2O	4.87	5.30	5.35	7.45	7.42	7.44	8.24
K_2O	0.32	0.45	0.40	0.64	0.82	0.89	0.62
FeO	0.49	0.37	0.50	0.17	0.29	0.18	0.05
Total	98.73	99.98	99.33	99.99	98.14	98.04	99.21
An	55.8	51.9	50.8	34.6	30.9	27.8	25.8
Ab	42.4	45.5	46.8	61.9	64.4	66.9	70.7
Or	1.8	2.6	2.4	3.5	4.7	5.3	3.5

gioclase. The plagioclase grains are either elongated (1:3), inequigranular and fractured, or have irregular subisometric forms. Most of the grains are resorbed wholly or along concentric zones. The lava flows of different ages were found to contain plagioclase of several generations.

Melt inclusions in plagioclase can be classified into two types. Inclusions of the first type are restricted to resorption zones and have the form of "channels" or closed irregular dark glass inclusions. Those of the second type are included into translucent grain regions, are usually rounded, and are composed of light-color glass with a perfectly visible gas bubble, and are wholly or partially crystallized.

Quartz is present in rounded, often fractured grains. Its melt inclusions are usually glassy, isometric, rounded, or square with smoothed angles.

The melt inclusions may be restricted to any grain region and are distinguished by clear-cut contacts (usually rectilinear with smoothed angles) and large sizes. They are composed of light-color glass without any indications of crystallization.

After the polished plates had been examined under the microscope, the phenocrysts with their melt inclusions were

Table 8. Chemical compositions (wt. %) of melt inclusion glasses in the minerals of the Elbrus rocks

Sample no.	Component												Total	T, °C	An
	SiO_2	TiO_2	Al_2O_3	FeO	MnO	MgO	CaO	Na_2O	K_2O	P_2O_5	Cl	S			
25/97	57.52	1.02	18.17	4.45	0.00	2.67	4.89	3.54	4.50	0.55	0.05	0.05	97.41	1120	56
36/97	60.10	1.35	18.99	4.62	0.02	3.18	3.78	5.23	2.63	0.23	0.17	0.04	100.34	1120	47
44/97	60.77	0.42	17.65	1.59	0.04	0.31	3.40	3.28	5.35	0.03	0.03	–	92.87	1000	51
36/97	62.49	0.92	18.59	3.88	0.00	2.59	3.19	5.27	3.08	0.18	0.11	0.04	100.34	1120	47
25/97	65.41	0.31	19.95	0.69	0.03	0.11	1.78	5.35	5.32	0.01	0.21	0.03	99.20	1170/	29
50/97	66.77	1.20	13.80	3.99	0.05	1.20	2.39	3.16	4.93	0.21	0.06	0.04	97.80	1100	52
50/97	67.13	1.44	14.65	5.16	0.09	1.64	2.57	3.14	4.05	0.36	0.04	0.04	100.31	1100	52
25/97	69.27	0.01	17.84	0.40	0.04	0.03	1.21	4.22	6.42	0.00	0.03	0.04	99.51	1170	29
45/97	70.86	0.09	11.90	0.41	0.00	0.08	0.73	3.68	5.01	0.05	0.04	0.01	92.86	1130	28
47/97	71.43	0.03	16.06	0.52	0.08	0.06	1.18	4.79	5.82	0.04	0.11	0.00	100.12	1000	Q
34/97	71.54	0.48	13.56	2.01	0.05	0.52	1.22	3.43	3.83	0.11	0.10	0.02	96.91	1130	48
45/97	72.43	0.24	12.81	0.46	0.00	0.13	0.54	3.02	5.75	0.01	0.07	0.01	95.47	20	31
45/97	73.04	0.35	13.31	0.93	0.03	0.20	0.86	3.40	5.58	0.02	0.03	0.02	97.77	1130	28
25/97	73.40	0.08	14.78	0.30	0.06	0.12	0.87	3.84	6.06	0.01	0.06	0.02	99.60	1120	Q
45/97	74.91	0.39	11.16	0.71	0.11	0.11	0.61	3.17	5.09	0.03	0.10	0.01	96.40	20	31
34/97	76.12	0.05	11.73	0.28	0.04	0.02	0.44	3.91	4.81	0.02	0.08	0.02	97.52	1130	Q
36/97	76.91	0.04	12.18	0.38	0.03	0.04	0.51	3.51	3.00	0.00	0.05	0.02	96.67	1120	Q
34/97	76.88	0.09	11.82	0.34	0.05	0.01	0.47	3.04	4.45	0.03	0.05	0.03	97.26	20	Q
34/97	77.47	0.05	11.66	0.45	0.05	0.04	0.36	3.04	4.98	0.01	0.04	0.02	98.17	20	Q
25/97	78.06	0.06	12.52	0.45	0.01	0.07	0.54	3.38	4.95	0.05	0.01	0.04	100.14	1170	29
34/97	80.08	0.05	11.06	0.44	0.00	0.06	0.38	3.30	4.49	0.01	0.05	0.02	99.94	20	Q

Note. FeO denotes total iron, An, the composition of the host plagioclase, and Q, the host mineral (quartz).

Table 9. Chemical compositions (wt.%) of Elbrus and Kazbek magmatic melts

Component	Melt inclusions in minerals				Melt		
	Elbrus			Kazbek	Elbrus		Kazbek
	andesite	dacite	rhyolite	rhyolite	dacite	rhyolite	rhyolite
SiO_2	60.22	68.80	75.93	75.32	67.64	76.43	73.48
TiO_2	0.93	0.45	0.14	0.26	0.12	0.12	0.78
Al_2O_3	18.35	15.91	12.30	13.38	17.13	12.02	13.76
FeO	3.64	1.78	0.47	0.94	1.01	0.54	2.54
MnO	0.02	0.04	0.04	0.02	0.02	0.02	0.01
MgO	2.19	0.47	0.08	0.12	0.20	0.04	0.46
CaO	3.82	1.55	0.56	0.68	1.71	0.56	2.30
Na_2O	4.33	4.07	3.36	4.51	3.42	2.52	3.01
K_2O	3.89	5.16	4.92	3.28	7.40	6.16	3.24
P_2O_5	0.25	0.11	0.02	0.09	0.03	0.02	n.d.
Cl	0.09	0.08	0.05	0.17	0.06	0.10	0.06
S	0.04	0.03	0.02	0.03	0.01	0.01	0.03
Total	97.77	98.45	97.89	98.77	98.75	98.54	99.67
K_2O/Na_2O	0.90	1.27	1.46	0.73	2.16	2.44	0.93
n	4	8	10	11	6	4	7

Note. FeO denotes total iron, (n) is the number of measurements, n.d. – not determined.

heated in a micromuffle with a platinum heater [*Naumov,* 1969] to temperatures of 1000–1170°C (homogenization temperature of the smallest grains) and then were quenched. The minimum heating time was 1.5 hours, the maximum, 4 hours. After their quenching the melt inclusions were brought to the surface of the crystals and then analyzed using a Camebax Microbeam electron microanalizer under the following conditions: accelerating voltage of 15 kV, current of 30 Na, with the optical raster sweep of 12×12, 5×5, and 2×2 μm during the study of glasses, and 2×2 μm during the identification of crystalline phases. The accuracy of determining chemical elements was roughly 10±2 wt%, about 5 % in the case of their content being 5–10 wt %, and about 10 % in the case of their contents being 1–5 wt. %. It should be noted that the analyses of glass inclusions in the case of scanning small areas showed a substantial loss of Na, this fact having been recorded earlier [*Naumov et al.,* 1990; *Tolstykh et al.,* 1998, 1999, 2001].

The following technique was used for getting more accurate Na contents: in the case of large glass inclusions (∼30–50 μm) glasses were analyzed using different scanning areas. This allowed us to compute corrections for Na values in the case of small melt inclusions.

The compositions of glasses from melt inclusions in the minerals of the Elbrus rocks are listed in Table 8.

The melt inclusions in the minerals of the Elbrus volcanic rocks vary significantly in the silica content, from 57.5 to 80.1 wt. %, most of them being rhyodacite-trachyriodacite (69.2 to 73.0 wt. % SiO_2) and rhyolite-trachyrhyolite (73.4–80.0 wt % SiO_2). There is a certain correlation between the contents of some petrogenic elements and silica. For instance, as the melt becomes less basic, the contents of some elements decrease as follows (in wt. %): 1.4 to 0.3% Ti, 20.0 to 11.1% Al, 4.6 to 0.3% Fe, 3.2 to 0.01% Ma, and 4.9 to 0.4% Ca. The trends of decreasing Na_2O contents and increasing K_2O contents are less distinct.

While dealing with the origin of andesite magma, we generalized all data available in the literature (85 analyses of andesite and 317 analyses of melt inclusions in phenocrysts from these rocks). *Naumov et al.* [1997] showed that most of the world andesites had been produced during the crystallization of dacite and rhyolite magmas. In this case andesite is a cumulate rock, the basic nature of which being the result of the mixing of more acid magma and less basic phenocrysts.

All data derived in this study for the chemical composition of melt inclusions in the Elbrus minerals and groundmass can be classified definitely into the following groups in accordance with the conventional classification of igneous rocks based on their SiO_2 contents (in wt. %): <63, 63–72, and >72.

The results presented in Table 9 suggest the presence of three types of magmas that had existed during the crystallization of plagioclase and quartz in the dacite of Elbrus Volcano, that is, trachyandesite, trachydacite, and trachyrhyolite magmas. One can clearly see the natural variations in the contents of petrogenic elements with the growth of the silica contents of magma and the declining contents of TiO_2, Al_2O_3, FeO, MgO, and CaO.

Content of phosphorus, chlorine, sulphur decrease and K_2O/Na_2O relation value increases (from 0.90 to 1.46) in the melt. High concentration of potassium (6.2–7.4 wt %), is characteristic of the glass in matrix, and therefore K_2O/Na_2O relation in them amounts to 2.16–44.

The data obtained we consider as the beginning of complex investigations that allow to reveal the evolution of magmatism and mixing of the melts of different composition of the Elbrus – the largest volcano of this region.

Acknowledgments. This research was financially supported by the Russian Foundation for Basic Research (project nos. 03-05-64215, 03-05-96744).

References

Babanskii, A. D., N. A. Ashikhmina, V. I. Kovalenko, et al. (1995), Parental magma for the rocks of the Upper Chegem Caldera (North Caucasus) from the results of studying inclusions in the minerals, *Dokl. Rus. Akad. Nauk, 344*(2), 226–228.

Belyaev, G. M., and V. A. Rudnik (1978), *Genetic Types of Granites,* pp. 67–74, Nedra, Leningrad.

Bogatikov, O. A., I. V. Melekestsev, A. G. Gurbanov, et al. (1998a), Catastrophic Paleolahars of the Elbrus Volcano (North Caucasus), *Dokl. Russ. Acad. Nauk, 362*(4), 518–521.

Bogatikov, O. A., I. V. Melekestsev, A. G. Gurbanov, et al. (1998b), Radiocarbon dating of Elbrus Holocene eruptions (North Cauasus, Russia), *Dokl. Russ. Akad. Nauk, 363*(2), 219–221.

Borsuk, A. M. (1979), *Mesozoic and Cenozoic Igneous Rock Formations of the Greater Caucasus,* 299 pp., Nauka, Moscow.

Chappell, B. W., and A. J. R. White (1974), Two contrasting granite types, *Pac. Geol., 8,* 173–174.

Chernyshev, I. V., V. A. Lebedev, S. N. Bubnov, et al. (2001), Stages in the magmatic activity of the Elbrus volcanic center from the study of inclusions in minerals, *Dokl. Ros. Akad. Nauk, 380*(3), 384–389.

Dotduev, S. I. (1975), Alignment surfaces at the northern slope of the Central Caucasus, *Proc. Azerbaidzhan University, ser. Geol. and Geogr. Nauk,* (5/6), 44–56.

Dotduev, S. I., and N. A. Lebedeva (1981), On volcanogenic-debris deposits of the city Georgievsk area and age of rhyolite composition tuffs and ignimbrites of the Central Caucasus, *Bull. Commit. Invest. Quartern. Period,* (51), 154–159.

Frost, B. R., G. G. Barnes, W. J. Collins, et al. (2001), A geochemical classification for granitic rocks, *J. Petrol., 42*(11), 2033–2048.

Ivanov, D. A., S. N. Bubnov, V. M. Volkova, et al. (1993), Sr and Nd isotope composition of Quaternary lavas in the Great Caucasus region in terms of their petrogenesis, *Geokhimiya,* (3), 343–353.

Kozlov, V. D. (1977), *Petrochemistry, Geochemistry, and Ore Content of Granites in the Central Transbaikal Region,* 253 pp., Nauka, Novosibirsk.

Koronovskii, N. V. (1968), Geologic Structure and Evolution of the Elbrus Volcano, in *Elbrus Glaciation,* pp. 15–74, Moscow University Press, Moscow.

Koronovskii, N. V., and L. M. Rudakov (1962), Dating of the last Elbrus eruptions, in *Proc. Education Institutions, Ser. Geology and Exploration,* no. 8, 133–135.

Lazarenko, K. A., and K. A. Deichakovskaya (1973), Miocene mixed rhyolite and andesite tuffs and lavas in the Transcarpathian region, in *Volcanism and the Formation of Mineral Deposits in the Alpine Geosynclinal Zone (Carpathian, Crimea, and Caucasus Regions),* pp. 153–163, Nauka, Novosibirsk.

Markhinin, E. K. (1964), Calderas and peripheral volcanic chambers, in *Proc. Laboratory of Paleovolcanology,* no. 3, pp. 138–147, Kazakh. Research Institute of Mineral Resources.

Masurenkov, Yu. P. (1961), *Cenozoic Volcanism in the Elbrus Volcanic Region,* 132 p., Moscow.

Naumov, V. B. (1969), A thermometric study of melt inclusions in quartz phenocrysts from quartz porphyry, *Geokhimiya,* (4), 494–498.

Naumov, V. B., V. I. Kovalenko, A. D. Babanskii, and M. L. Tolstykh (1997), The genesis of andesite reconstructed from studying melt inclusions in minerals, *Petrologiya, 5*(6), 654–665.

Naumov, V. B., I. P. Solovova, V. I. Kovalenko, and A. V. Guzhova (1990), Crystallization of topaz, albite, potassium feldspar, mica, and columbite from ongonite melt, *Geokhimiya,* (8), 1200–1205.

Popov, V. S. (1981), Magma mixing during the formation of recent volcanics in the Caucasus region, *Volcanology and Seismology,* (1), 3–13.

Rozen, O. M., and V. S. Fedorovskii (2001), *Collision Granitoids and Crustal Layering,* 188 pp., Nauch. Mir, Moscow.

Sheimovich, V. S. (1979), *Kamchatkan Ignimbrites,* 177 pp., Nedra, Moscow.

Stankevich, E. K. (1976), *Recent Magmatism in the Greater Caucasus Region,* 232 pp., Nedra, Leningrad.

Sun, S. S., and W. F. McDonough (1989), Chemical and isotopic systematics of oceanic basalts: Implications for mantle composition and processes, Magmatism in the Ocean Basins, London, *Geol. Soc. Spec. Publ., 42,* 313–345.

Tolstykh, M. L., V. B. Naumov, A. D. Babanskii, et al. (1998), The melt composition and crystallization conditions of Shiveluch Volcano andesite (Kamchatka) from the study of inclusions in minerals, *Dokl. Russ. Akad. Nauk, 359*(5), 676–679.

Tolstykh, M. L., V. B. Naumov, I. V. Bogoyavlenskaya, and N. N. Kononkova (1999), Andesite-dacite-rhyolite melts during andesite phenocryst crystallization in Bezymyannyi Volcano, Kamchatka, *Geokhimiya,* (1), 14–24.

Tolstykh, M. L., V. B. Naumov, A. G. Gurbanov, et al. (2001), The composition of Elbrus and Kazbek magmas from the study of inclusions in minerals, *Geokhimiya,* (4), 441–448.

Vinogradov, A. P. (1962), Average contents of chemical elements in the main types of crustal igneous rocks, *Geokhimiya,* (7), 555–557.

A. G. Gurbanov, V. M. Gazeev, O. A. Bogatikov,
A. Ya. Dokuchaev, Institute of Geology of Ore Deposits,
Petrography, Mineralogy and Geochemistry, Russian Academy of Science, 35 Staromonetny, Moscow, Russia

V. B. Naumov, Vernadsky Institute of Geochemistry and Analytical Chemistry, Moscow, Russia

A. V. Shevchenko, Kabardino-Balkarian University

(Received 24 August 2004)